

## Characterization of domain specific Interaction of Synthesized Dye with Serum Proteins by Spectroscopic and Docking Approaches along with Determination of Invitro Cytotoxicity and Antiviral Activity

Suparna Rudra, Somnath Dasmandal, Chiranjit Patra, Biman Kumar Patel, Suwendu Paul & Ambikesh Mahapatra

To cite this article: Suparna Rudra, Somnath Dasmandal, Chiranjit Patra, Biman Kumar Patel, Suwendu Paul & Ambikesh Mahapatra (2017): Characterization of domain specific Interaction of Synthesized Dye with Serum Proteins by Spectroscopic and Docking Approaches along with Determination of Invitro Cytotoxicity and Antiviral Activity, Journal of Biomolecular Structure and Dynamics, DOI: [10.1080/07391102.2017.1400468](https://doi.org/10.1080/07391102.2017.1400468)

To link to this article: <http://dx.doi.org/10.1080/07391102.2017.1400468>



Accepted author version posted online: 01 Nov 2017.



Submit your article to this journal [↗](#)



View related articles [↗](#)



View Crossmark data [↗](#)

**Publisher:** Taylor & Francis

**Journal:** *Journal of Biomolecular Structure and Dynamics*

**DOI:** <http://doi.org/10.1080/07391102.2017.1400468>



**Characterization of domain specific Interaction of Synthesized Dye with Serum Proteins by Spectroscopic and Docking Approaches along with Determination of Invitro Cytotoxicity and Antiviral Activity**

Suparna Rudra<sup>a</sup>, Somnath Dasmandal<sup>a</sup>, Chiranjit Patra<sup>a</sup>, Biman Kumar Patel<sup>a</sup>, Suvendu Paul<sup>b</sup> and Ambikesh Mahapatra<sup>a,\*</sup>

<sup>a</sup>*Department of Chemistry, Jadavpur University, Kolkata 700 032, India*

<sup>b</sup>*Department of Chemistry, Kalyani University, Kalyani 741235, India*

\*Corresponding author, Tel.: +91 33 2457 2770 (Office); +91 33 2432 4586 (Residence);  
Facsimile: +91 33 2414 6223

*e-mail addresses:* [ambikeshju@gmail.com](mailto:ambikeshju@gmail.com) & [amahapatra@chemistry.jdvu.ac.in](mailto:amahapatra@chemistry.jdvu.ac.in)

**Abstract**

The interaction between a synthesized dye with proteins, bovine and human serum albumin (BSA, HSA respectively) under physiological conditions has been characterized in details, by

means of steady state and time resolved fluorescence, UV-Vis absorption and circular dichroism (CD) techniques. An extensive time-resolved fluorescence spectroscopic characterization of the quenching process has been undertaken in conjunction with temperature-dependent fluorescence quenching studies to divulge the actual quenching mechanism. From the thermodynamic observations, it is clear that the binding process is a spontaneous molecular interaction, in which van der Waals and hydrogen bonding interactions play the major roles. The UV-Vis absorption and CD results confirm that the dye can induce conformational and micro environmental changes of both the proteins. In addition, the dye binding provoke the functionality of the native proteins in terms of esterase-like activity. The average binding distance ( $r$ ) between proteins and dye has been calculated using FRET. Cytotoxicity and antiviral effect of the dye has been found using Vero cell and **HSV-1F** virus by performing MTT assay. The AutoDock-based docking simulation reveals the probable binding location of dye within the sub domain IIA of HSA and IB of BSA.

*Keywords:* Azo dye, serum albumin, docking, fluorescence

## **1. Introduction**

In modern era there is a phenomenal rise in the growth of different organic dyes owing to their extensive uses in different industries like food, textile, printing, cosmetics, electronics and

pharmaceuticals. Apart from these commercial uses, dyes are also used as probe for understanding the mechanism of different photo physical processes. (Carter et. al., 1994) Among different types of dyes, water soluble azo dyes are extensively employed in foodstuff like swiss rolls, jams, jellies, yoghurts, breadcrumbs; mouthwash and cheese cake mixes etc (Amin et.al., 2010). However most of these dyes have been found to have carcinogenic effects on human body that may cause bladder cancer, splenic sarcomas, hepatocarcinomas and nuclear anomalies in animal models (Medvedev et. al., 1988). The cleavage of azo linkage leads to the development of a highly toxic carcinogenic molecule benzidine which can adversely affect our urinary organs, stomach, kidney, brain, and liver (Ratna et. al., 2012). As they are toxic, carcinogenic, mutagenic and less degradable, the effluent discharged by the textile industries after dyeing process is concerned as a pollutant (Chowdhury et. al., 1996). The physiological and toxicological actions of the dyes are related to the binding capacity of the proteins.

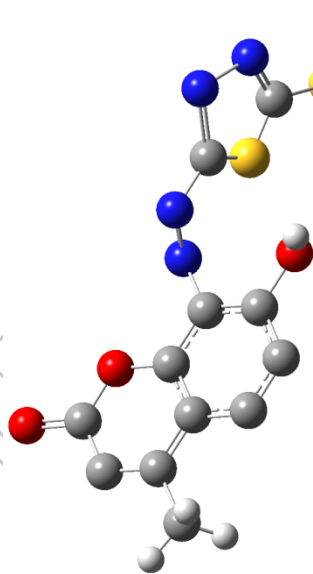
Biomacromolecules such as proteins, nucleic acids have very much important role in living systems. Serum albumins, one of the most plentiful compounds in the blood plasma are the major constituent of the circulatory system. They expedite the transport process and delivery of various exogenous and endogenous ligands including long-chain fatty acids, drugs and metal ions (Xu et. al., 2012). Serum proteins are also responsible for maintaining colloid blood pressure and are extremely effective for biological functions like membrane preparation, metabolism and other pharmacokinetic properties (Khan et. al., 2012).

The well-known serum proteins Bovine Serum albumin (BSA) and Human Serum Albumin (HSA) have formed the center of many-faceted research activities for years. Apart from their abundance and ease of purification, the intense importance of them in pharmaceutical industries originating from its functional properties has played a foremost role in modern research area.

These most abundant multifunctional proteins in Bovine and Human blood respectively have almost 76% structural similarity (Peters, 1996). The primary structure of BSA contains 583 amino acids and that of HSA contains 585 amino acid residues. From determined crystallographic structure of the proteins it is proposed that single Tryptophan residue (Trp-214) of HSA is located in IIA binding site and in case of BSA two tryptophan moieties *viz.* Trp-213 and Trp-134 are present in hydrophobic sub domain IIA and less hydrophobic IA respectively (Sudlow et. al., 1975; Arumugam et.al., 2016) The tertiary structure of them is constituted of almost 67% helical content and 17 disulphide bridges (Peters, 1985). In pharmaceutical industries it is accepted that the overall distribution and metabolism of different ligands can be altered on the basis of their affinity to proteins. In addition, many drug molecules are considered as ineffective owing to their high affinity towards proteins. So, different types of interaction of various biologically active compounds with proteins advocate new approach to drug therapy and design (Roy et. al., 2017; Qin et al., 2016).

Coumarin derivatives are very much important to the modern drug designers owing to that most of them have antimicrobial, anti-inflammatory, antitumor and anticancer activity. For this vast range of application they are widely used in pharmaceutical industries. Coumarins are strongly fluorescent and have high photo stability, so that they are extensively used in cosmetic world. Normally most of the coumarin compounds are colorless but substitution at different position make them colorful and used in the application such as laser dyes, textile dyes etc (Chen et. al., 2013; Bayraktutan et. al., 2017; Akbaya et. al., 2010; Vaarla et.al., 2015; Christie et. al., 2008). Consequently, in our present investigation we have tried to design a coumarin based azo dye having antiviral effect as well as protein binding capacity which can be applicable in cosmetics, textile and pharmaceutical industries. To focus on its protein binding capacity (with two plasma

proteins BSA and HSA) various spectroscopic techniques have been asserted. Herein, the dye-protein binding phenomenon has been observed by steady-state and time-resolved fluorescence spectroscopy in which the dye induced quenching of the intrinsic fluorescence of the proteins has been monitored to elucidate the binding strength. For precise evaluation of therapeutic activity of the synthesized dye on proteins, absorption and circular dichroism studies have been done. Cytotoxicity and antiviral effect of the dye has been found using Vero cell and **HSV-1F** virus by performing MTT assay. We have introduced a computational approach to establish the binding location of the dye around the macromolecular architecture of the serum proteins in order to provide theoretical support to the experimental findings.



Scheme 1: Structure of the synthesized azo dye

## 2. Materials and methods

### 2.1. Materials

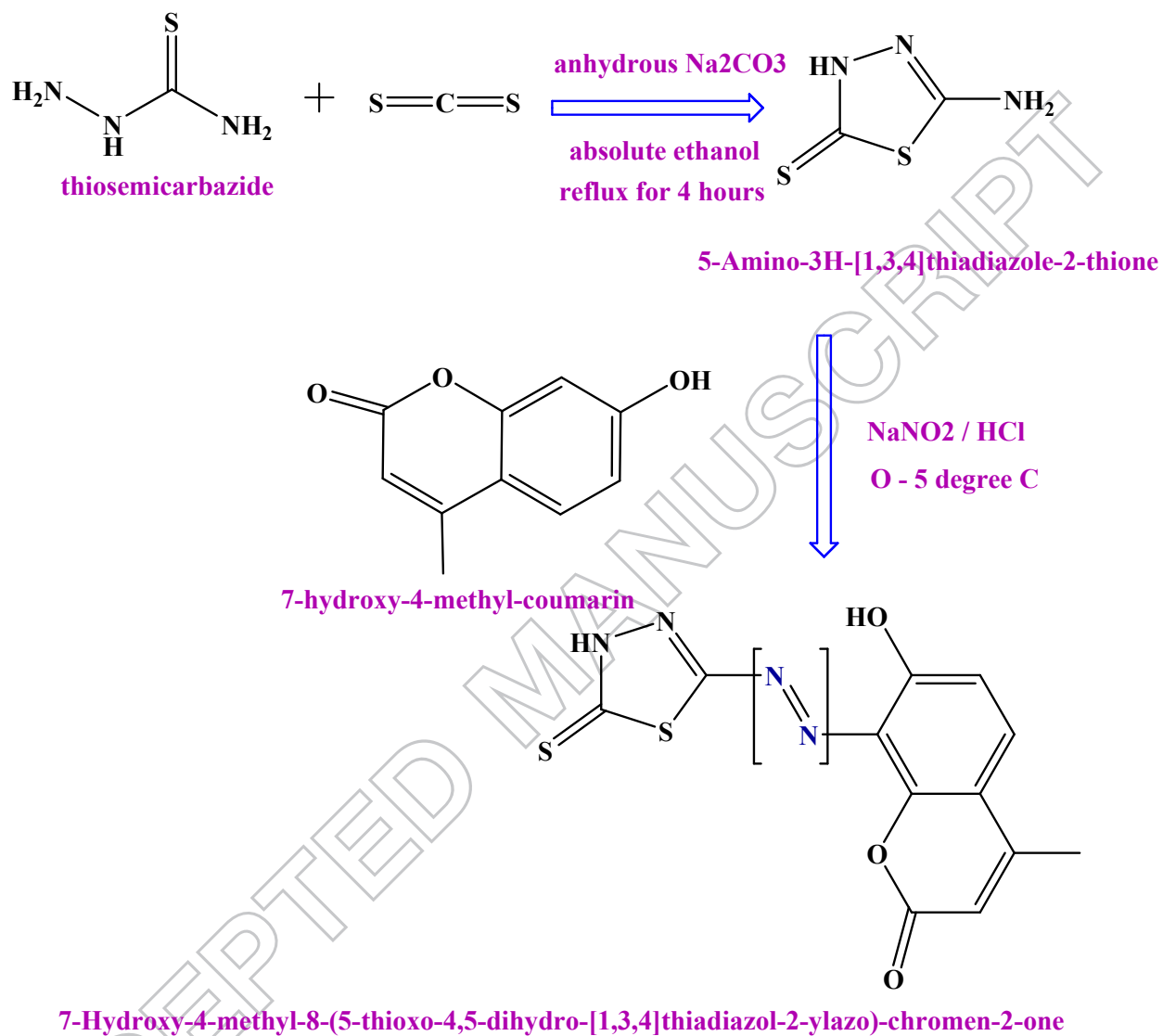
Thiosemicarbazide (puriss. p.a., 98%), carbon disulphide, anhydrous sodium carbonate (anhydrous, free-flowing, Redi-Dri™, ACS reagent, ≥99.5%), bovine serum albumin (BSA) and

human serum albumin (HSA) (lyophilized powder,  $\geq 97\%$  (agarose gel electrophoresis)) have been purchased from Sigma Aldrich (USA) and used as received. All other chemicals have been procured from the commercial sources as per requirements and used after purification. The sample solutions have been prepared in 10 mM *tris*- HCl/10 mM NaCl buffer (pH = 7.4) using deionized ultrapure water from Millipore Synergy System (Merck, India). The *tris* base has been purchased from Merck, India. Stock solution of BSA and HSA have been prepared in 10 mM *tris*- HCl buffer measuring the absorbance at 280 nm with  $\epsilon$  value of 43,824 M<sup>-1</sup> cm<sup>-1</sup> and 42,864 M<sup>-1</sup> cm<sup>-1</sup> respectively (Peters, 1975; Andrade et.al., 2002). All the protein solution have been stored in the dark at 4 °C and used within 4 days. Stock solution of dye has been prepared by methanol-water (1:9) mixture system due to its low solubility in water.

## 2.2. Synthesis of Azo dye

5-Amino-3H-[1, 3, 4] thiadiazole-2-thione has been prepared according to a literature method (Popiołek et. al., 2015). To (1.33 g, 0.01 mol) of 5-Amino-3H-[1, 3, 4]thiadiazole-2-thione taken in a 500-mL RB flask 60 mL of 50% HCl solution has been added and it was stirred at 0 -5 °C. To this solution an ice-cold solution of sodium nitrite (0.828 g, 0.012 mol) has been added at a rate such that the temperature should not rise above 5 °C. The cold diazonium chloride solution thus prepared has been added very slowly with vigorous stirring to cold (0 °C) alkaline 7-hydroxy-4-methyl-coumarin (1.76 g, 0.01 mol) in a 250-mL RB flask immersed in an ice salt bath. The reddish brown solid separated was filtered, washed with water, dried, and collected with 60 %Yield (~ 2.0 g). Microanalytical data : C<sub>12</sub>H<sub>8</sub>N<sub>4</sub>O<sub>3</sub>S<sub>2</sub>; Calcd. (Found): C, 44.99 (44.98); H, 2.52 (2.53); N, 17.49 (17.51) %. <sup>1</sup>H-NMR (300 MHz, CDCl<sub>3</sub>).  $\delta$  10.53 (s, H, OH<sub>a</sub>) , 6.11 (s, H, H<sub>b</sub>), 6.69 (s, H, H<sub>c</sub>), 6.78 (d, H, J = 12, H<sub>d</sub>), 6.58 (d, H, J = 9, H<sub>e</sub>), 2.34 (s, 3H, H<sub>f</sub>). IR: 3492.51 cm<sup>-1</sup> (phenolic -O-H), 1667.41 cm<sup>-1</sup> (-C=N), 1455.29 cm<sup>-1</sup> (azo, -N=N). (NMR and IR

spectra have been shown at Figs. S1 and S2, S stands for supporting information).



Scheme 2: Synthesis of (7-Hydroxy-4-methyl-8-(5-thioxo-4, 5-dihydro-[1, 3, 4]thiadiazol-2-ylazo)-chromen-2-one)

### 2.3. Protein binding experiment:

#### 2.3.1. Absorption Studies:

UV-Vis absorption spectroscopy has been employed to investigate the interactive phenomena

between the synthesized dye and serum albumins using UV-Vis Spectrophotometer (Shimadzu, UV-1800) equipped with a Peltier temperature controller, TCC-240A in order to sustain a constant temperature of 298 K ( $\pm 0.1$  K). A quartz cell from Hellma of 1 cm path length has been used in this study. The dye solution has been added to the fixed amount of buffered protein solution and during addition of the dye an equal amount of it has been added to both sample and reference cell in order to cancel out the contribution of the added dye to the absorbance of protein spectra.

### **2.3.2. Steady state fluorescence spectroscopy**

Steady-state fluorescence measurements have been carried out on a Shimadzu RF-5000 spectrofluorimeter. The intrinsic fluorescence of proteins has been studied upon exciting at 295 nm using excitation and emission band slits of 5 nm each. The effect of proteins on dye fluorescence has also been studied upon exciting the dye at 320 nm. During fluorometric titration experiments, the dilution factor of the dye has been corrected.

### **2.3.3. Time resolved fluorimetric analysis**

Fluorescence lifetimes of Trp in albumin proteins have been determined from time-resolved intensity decays by employing time-correlated single-photon-counting (TCSPC) technique using Horiba Jobin Yvon at 298 K. A nanosecond diode laser at 300 nm (IBH UK) has been used as an excitation source with a TBX photon detector and the signals have been recorded at the magic angle of  $54.7^\circ$ . The number of counts gathered in the channel of maximum intensity has been fixed at 2500. The data have been analyzed using a nonlinear least-squares iterative method utilizing the Fluorescence Analysis Software IBH DAS-6. The quality of fits has been judged from  $\chi^2$  (0.9 ~ 1.2) data (Lakowicz, 2006). The following equation (1(a)) (Lakowicz, 2006) has

been used to investigate the experimental time-resolved fluorescence decays where,  $F(t)$  is the fluorescence intensity at time  $t$  and  $\alpha_i$  is the pre-exponential factor representing the fractional contribution to the time-resolved decay of the  $i^{\text{th}}$  component with a lifetime  $\tau_i$ . For multiexponential decays, the average lifetime has been calculated from the following equation where ( $\tau_1$ ,  $\tau_2$  and  $\tau_3$ ) are decay times and ( $\alpha_1$ ,  $\alpha_2$  and  $\alpha_3$ ) are the normalized pre-exponential factors.

$$F(t) = \sum_i a_i \exp\left(\frac{-t}{\tau_i}\right) \quad (1(a))$$

$$\alpha_1\tau_1 + \alpha_2\tau_2 + \alpha_3\tau_3 = \langle\tau\rangle \quad (1(b))$$

#### 2.3.4. Circular dichroism Studies:

Circular dichroism spectra of the albumins have also been recorded in presence and absence of azo dye owing to explain the conformational properties of proteins upon action of dye using a JASCO J-815 spectropolarimeter attached to a water bath to control the temperature of the electronic circuit. The concentration of albumins has been kept at 0.4  $\mu\text{M}$  for instrumental requirement. The CD results have been expressed in terms of mean residue ellipticity (MRE) in  $\text{deg cm}^2 \text{dmol}^{-1}$  using eq. 2 (Kelly et. al., 2005).

$$\text{MRE} = \theta_{\text{obs}} / 10 n l [\text{P}] \quad (2)$$

Where  $\theta_{\text{obs}}$  is the CD in millidegree,  $n$  is the number of amino acid residue (583 for BSA, 585 for HSA),  $l$  is the optical path length of the cell,  $[\text{P}]$  is the molar concentration of the albumin. CD spectra have been recorded in the wavelength range of 200 - 275 nm with scan speed of 50  $\text{nm min}^{-1}$ . An average of three scans has been done for each spectrum at 298 K. The base line has been subtracted from each data set.

### 2.3.5. Esterase activity assay

The effect of dye on the esterase activity of serum proteins toward *p*-nitrophenyl acetate (*p*-NPA) has been analyzed on a Shimadzu, UV-1800 UV-Vis spectrophotometer by steady-state kinetics at 310 K. The concentration of albumins and *p*-NPA has been kept constant at 25  $\mu$ M and 50  $\mu$ M respectively. The rate of *p*-NPA hydrolysis has been determined by measuring the appearance of *p*-nitrophenol, a yellow product, at 400 nm for 500 s.

### 2.3.6. Cytotoxic activity assays and antiviral activity

One of the most well-known methods that used for the assessment of cell viability is the 3-[4, 5-dimethylthiazol-2-yl]-2, 5-diphenyltetrazolium bromide (MTT) assay based on the formation and colorimetric quantification of an enzyme activity (Mosmann, 1983, Mohamadi et. al., 2017).

MTT assay is a colorimetric method based on the rupturing of the yellow water-soluble tetrazolium salt, MTT, to form water insoluble, dark-blue formazan crystals. MTT splitting takes place only in living cells by mitochondrial succinate dehydrogenase enzyme. The formazan crystals are dissolved usually in *iso*-propanol or DMSO and the absorbance of the out-coming solution is measured using a spectrophotometer to calculate the concentration of the formazan, which is proportional to the number of viable cells. In our present contribution African green monkey kidney cells (Vero cell) morphology has been determined by MTT assay. Vero cells have been cultured onto 96-well plates at  $10 \times 10^6$  cells per well and different concentrations of the dye have been added to each well at a final volume of 100  $\mu$ L, in triplicate using DMSO (0.1%) and acyclovir (0–50  $\mu$ g mL<sup>-1</sup>) as a negative and positive control, respectively. The drug-treated cells have been incubated at 310 K with 5% CO<sub>2</sub> for 2 days and then the MTT reagent (10  $\mu$ L) has been added to each well. After 4 h of incubation, the formazan has been solubilized

by adding MTT solubilisation solution equal to the original culture media volume and the absorbance has been recorded at 570 nm with a reference wavelength of 690 nm by an ELISA reader. Data have been calculated as the percentage of cell viability by the formula.

Cell viability = [(sample absorbance cell free sample blank)/ mean media control absorbance]/ 100%.

In our present contribution the viral strains have been used as **HSV-1F** (ATCC 734), purchased from the ATCC (Manassas, VA, USA). Virus stocks have been prepared from infected culture at a multiplicity of infection (MOI) of 0.5 for 1 h at 310 K. The residual viruses have been then washed out with phosphate-buffered saline (PBS). We have determined the antiviral effects of the dye against HSV-1-infected Vero cells (MOI 1) by MTT assay, using acyclovir as positive and DMSO (0.1%) as negative control.

### 2.3.7. Theoretical Studies

Molecular simulation is beneficial to understand the interaction of drug molecules with serum albumin proteins combining to the experimental result. For docking analysis the ground state geometry of the synthesized azo dye has been optimized introducing density functional theory (DFT) in connection with B3LYP functional and 6-31G\* standard basis set in Gaussian 09 program suit (Koh et. al., 1965). The available crystal structures of the proteins have been collected from the protein data bank (PDB) with pdb id: 4F5S (BSA) and 4S1Y (HSA). The required pdb structure of the dye has been collected from the output file of the optimized structure. The dye has been docked using AutoDock 4.2 into the 3D structure of proteins (Morris, 1998). AutoDock 4.2 uses the Lamarckian genetic algorithm to investigate the optimum binding site of small molecules to the protein. To recognize the binding sites in serum albumins, docking has been done with the grid sizes 126, 126, and 126 along the x-, y-, and z- axes with a

0.675 Å grid spacing. The Auto Docking parameters have been used as follows: GA population size, 150; maximum number of energy evaluations, 250,000. During docking, a maximum of 50 conformers have been considered for each molecule, and the root mean square (rms) cluster tolerance has been set to 2.0Å. The output from AutoDock has been further analyzed using PyMOL software (Lano, 2004).

### 3. Results and Discussion

#### 3.1. Absorption Spectroscopic Study

UV-Vis absorption spectroscopy is an effective method in exploring the structural changes of the bio-macromolecules and to investigate protein-ligand complex formation. The UV-Vis absorption spectra of HSA in the absence and presence of dye obtained by utilizing the mixture of dye and *tris* buffer at the same concentration as the reference solution are shown in Fig. 1.

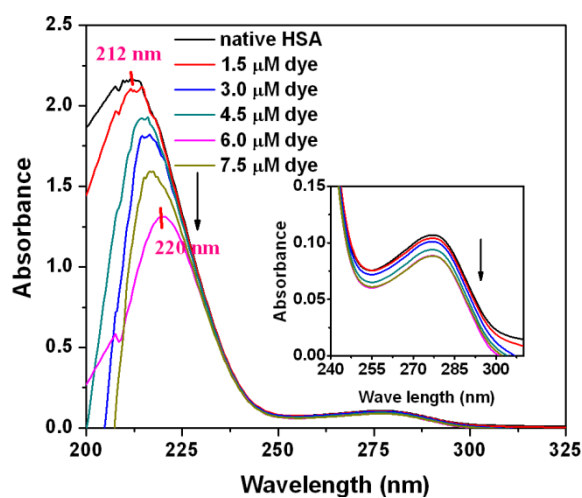


Fig. 1: UV-Vis spectra of HSA in presence of different concentrations of dye at 298 K and pH 7.4, [HSA] = 5 $\mu$ M, inset shows change of absorption spectra of protein at 278 nm upon action of dye

Albumins show two absorption peaks, the strong absorption peak at about 212 nm reflects the framework conformation of the protein, the weak one at about 278 nm appears to be due to the aromatic amino acids (Trp, Tyr, and Phe) (Zhao et. al., 2010; Lou et. al. 2017). Upon addition of the synthesized dye to the protein the intensity at 212 nm decreases with a red shift (212 to 220 nm for HSA and 211 to 222 nm for BSA) and the intensity of the peak at 278 nm have minimal changes (inset of Fig. 1). The results indicate that dye-protein interaction leads to increase the hydrophobicity of the microenvironment of the HSA (Pan et. al., 2011); similar phenomenon has been occurred in case of BSA also, which is not shown in the manuscript. Spectral changes in UV-Vis spectra of the albumins with addition of dye signify the presence of ground state complexation between them.

## **3.2. Fluorescence measurements**

### **3.2.1. Steady state fluorescence technique**

Fluorescence spectroscopy is a broadly applied technique for investigating protein conformation, dynamics and intermolecular interactions upon action of different drugs on it.

The intrinsic emission property of the proteins appears mainly due to presence of amino acid residues like Tryptophan (Trp), Tyrosin (Tyr) and Phenylalanine (Phe). However the

contribution of Phe to the total intrinsic fluorescence of Serum proteins is very low due to its low fluorescence quantum yields. Therefore any change in fluorescence property of Serum Albumin in presence of dye may be attributed due to the change occurring in the microenvironment of Trp and Tyr residues (Lakowicz, 2006).

The emission spectra of HSA and BSA have been recorded at  $\lambda_{em} = 340$  and  $346$  nm respectively in absence and presence of the dye (Fig. 2) upon excitation at  $295$  nm to avoid any contribution of Tyr residue and the resulting emission spectrum is exclusively ascribed to the intrinsic Trp fluorophore (Efink et. al., 1976).

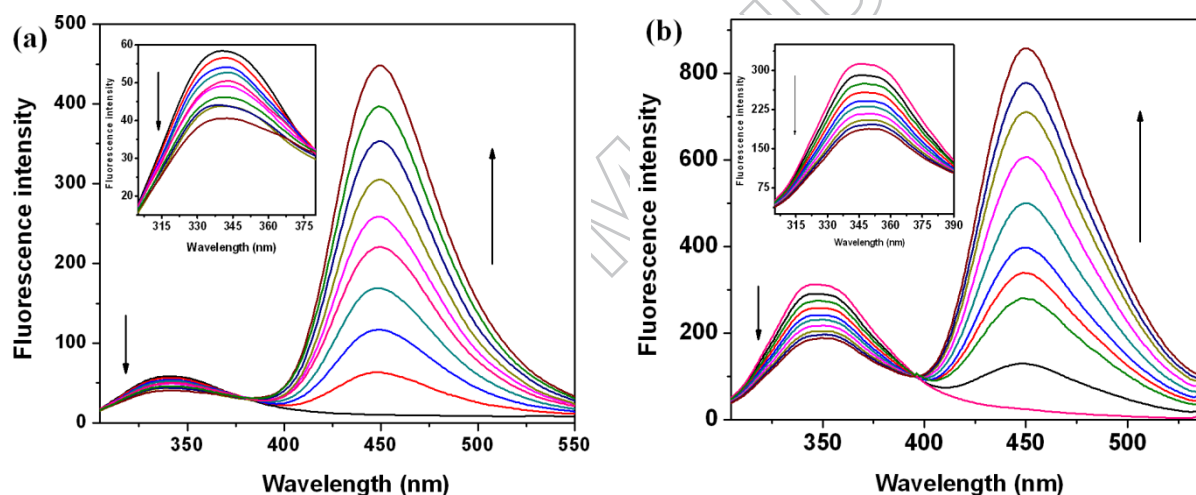


Fig. 2: Emission spectra of (a) HSA and (b) BSA at various concentration of azo dye. [dye] = 0, 0.75, 1.50, 2.25, 3.00, 3.75, 4.50, 5.25, 6.00, 6.75  $\mu\text{M}$ , [protein] = 5  $\mu\text{M}$ , inset shows change of protein fluorescence upon action of dye.

Fig. 2 illustrates that upon successive addition of dye, fluorescence intensity of the albumins decreases accompanying simultaneous enhancement in the fluorescence intensity of the dye at  $450$  nm. This is because of the fact that upon exciting the protein-dye mixture at  $295$  nm, some of the dye molecules get excited and thereby produces emission spectra centered at  $450$  nm. Such

decrease in fluorescence intensity of albumins implies that the dye can alter the structure of proteins. The dye induced structural changes of the proteins have been exemplified by slight red shift (340 to 342 nm for HSA and 346 to 348 nm for BSA) in emission spectra. It implies that the microenvironment across the amino acid residues of the proteins in vicinity of interaction site of the dye is perturbed, leading to greater extent of exposure of the Trp residue to the more polar aqueous milieu (Lakowicz, 2006). Such alteration of microenvironment near Trp residue indicates disruption of native structure of proteins upon action of the dye. Circular dichroic spectral responses of the proteins at presence of dye affix credence to the observations as discussed to the following sections.

### **3.2.2. Influence of Inner Filter Effect (IFE) on emission quenching of HSA/ BSA by the synthesized dye**

IFE refers to the absorption of light at the excitation or emission wavelength by the compounds present in the experimental solution. In the protein binding studies if ligand molecules possess strong absorption at the excitation wavelength of the protein, less light reaches to the centre of the sample and thus the emission intensity of the protein decreases, whereas, a strong absorption at the emission wavelength of protein would diminish the emitted light that reaches the detector. In our present investigation, the dye absorbs radiation at excitation wavelength of protein at 295 nm and emission wavelength at 340 nm for HSA and 346 nm for BSA (absorbance spectrum of the dye has been shown in Fig. S3). So, the IFE of the dye on the emission intensity of both HSA and BSA has been evaluated. Similar kind of observation has been reported for the binding interactions of  $\beta$ -conglycinin and glycinin with vitamin B12 (Dan et. al., 2007).

The emission intensities are corrected using the relationship, eq (3) (Lakowicz, 2006)

$$F_{corr} = F_{obs} \times e^{\frac{(A_{ex} + A_{em})}{2}} \quad (3)$$

Where,  $F_{corr}$  and  $F_{obs}$  are the corrected and observed emission intensities, respectively.  $A_{ex}$  and  $A_{em}$  are the solution absorbance at the excitation and emission wavelengths respectively.

The plots of  $(F/F_0)$  of both corrected emission intensities  $F_{corr}$  and observed emission intensities  $F_{obs}$  in case of HSA and BSA *versus* [dye] have been displayed in Fig. 3(a) and (b).

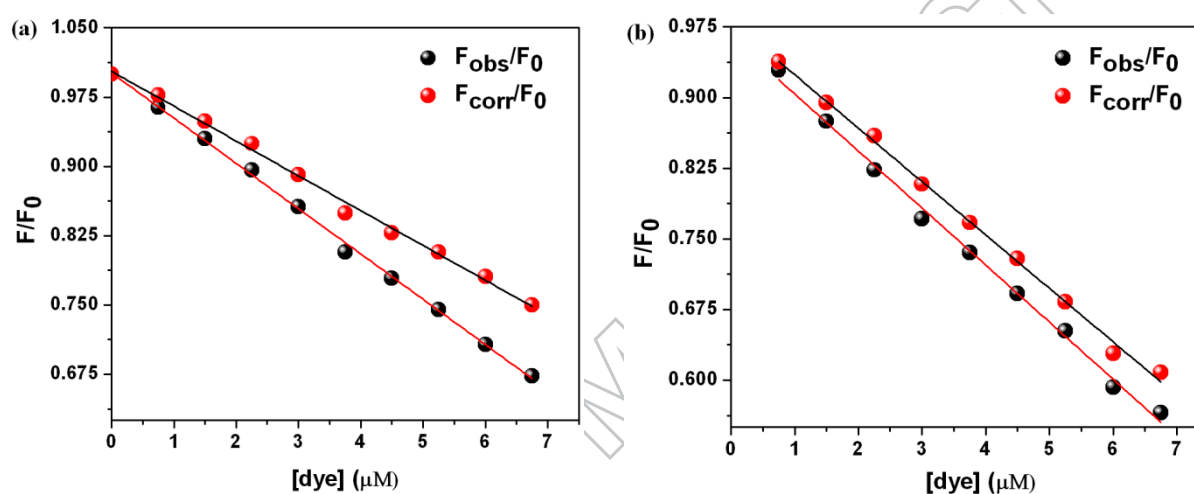


Fig. 3: Effect of inner filter effect (IFE) on the emission spectra of serum proteins for (a) HSA and (b) BSA at various dye concentration.  $[\text{dye}] = 0, 0.75, 1.50, 2.25, 3.00, 3.75, 4.50, 5.25, 6.00, 6.75 \mu\text{M}$ ,  $[\text{protein}] = 5 \mu\text{M}$ .

The  $(F/F_0)$  values of corrected and observed emission intensities decreased progressively with increase of dye concentration. The former is slower than the latter, signifying that the quenching of emission intensity of proteins is partly caused by IFE of dye. The decrease of corrected emission intensity of albumins due to presence of dye indicates presence of binding interaction between them.

In the present contribution our synthesized dye exhibits emission spectra at 450 nm upon excitation at 320 nm. We have studied the effect of proteins on fluorescence of the dye. The fluorescence intensity of dye decreases upon increment of protein concentration which implies the presence of drug-protein interaction (Fig. 4).

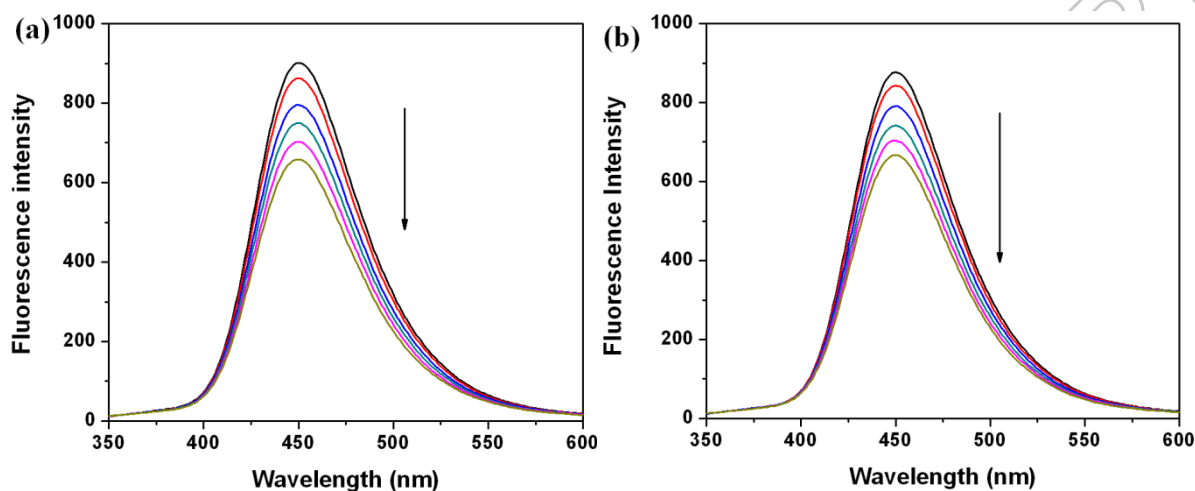


Fig. 4: Fluorescence emission spectra of azo dye in absence and presence of serum albumins, (a) HSA and (b) BSA {[dye] = 2  $\mu$ M, [serum albumin] = 2.5, 5.0, 7.5, 10.0, 12.5  $\mu$ M}. The arrow indicates the decrease in fluorescence intensity of the dye upon addition of albumins.

### 3.2.3. Quenching mechanisms of proteins in presence of dye

In modern science fluorescence technique has vast applications and this can be used to understand the mechanism of protein-ligand interaction. The quenching of emission spectra occurs mainly in two processes namely collisional or dynamic quenching through exciplex formation and static quenching due to ground state complexation (Lakowicz, 2006). As we have got the evidence of presence of ground state complexation between dye and proteins so the phenomenon of fluorescence quenching is conventionally described in terms of the well-known Stern–Volmer equation: (Lakowicz, 2006)

$$\frac{F_0}{F} = 1 + K_{sv} \frac{[Q]}{C^o} = 1 + k_q \tau_0 [Q] \quad (4)$$

Where,  $F_0$  and  $F$  are the corrected emission intensities of the proteins in absence and presence of quencher respectively.  $k_q$  is the bimolecular quenching constant,  $\tau_0$  is the average life time of fluorophore in absence of quencher and  $[Q]$  is the concentration of quencher.  $K_{sv}$  is the Stern-Volmer quenching constant indicating the efficiency of quenching.

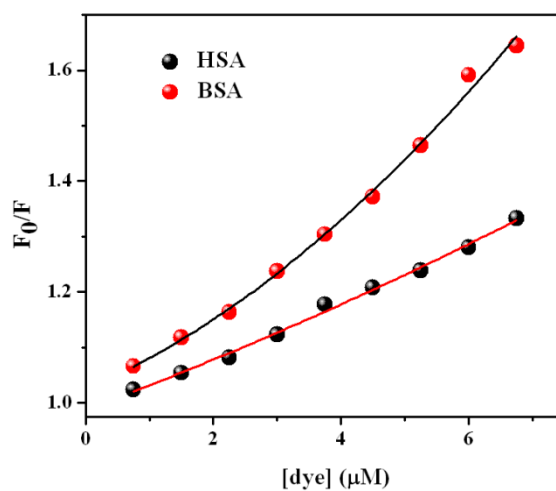


Fig. 5: Stern-Volmer plot of dye-serum protein system

According to the Stern-Volmer equation,  $F_0/F$  versus  $[dye]$  (Fig. 5) plot has been drawn for the quenching of serum proteins by the above mentioned dye. The plots show upward curvature to the Y axis (Adj. R square value ( $r$ ) = 0.9948 for HSA and 0.9944 for BSA) within the investigated concentration of dye. The nonlinearity of the curve implies the presence of both static and dynamic quenching by the same quencher (Lakowicz, 2006).

Therefore, modified Stern-Volmer equation has been used to analyze the quenching data. The equation helps in resolving the accessible and inaccessible residues when there is possibility of differential accessibilities of the proteins to the probe. The emission spectral studies have been analyzed according to the following modified Stern–Volmer equation (eq. (5)) (Lakowicz, 2006).

$$\frac{F_0}{\Delta F} = \frac{1}{f_a K_a} \frac{C^o}{[Q]} + \frac{1}{f_a} \quad (5)$$

Where,  $\Delta F$  is the difference in corrected emission intensity of HSA/ BSA in the absence and presence of quencher (dye)  $Q$ , ( $\Delta F = F_0 - F$ ),  $f_a$  is the fraction of accessible fluorescence and  $K_a$  is the effective quenching constant for the accessible fluorophores, which is analogous to the associative binding constant for HSA/ BSA–dye system. From Fig. 6 the plot  $F_0/\Delta F$  versus  $1/[dye]$  shows a linear relationship with a slope equal to  $C^o (f_a K_a)^{-1}$  and intercept equal to  $1/f_a$ .

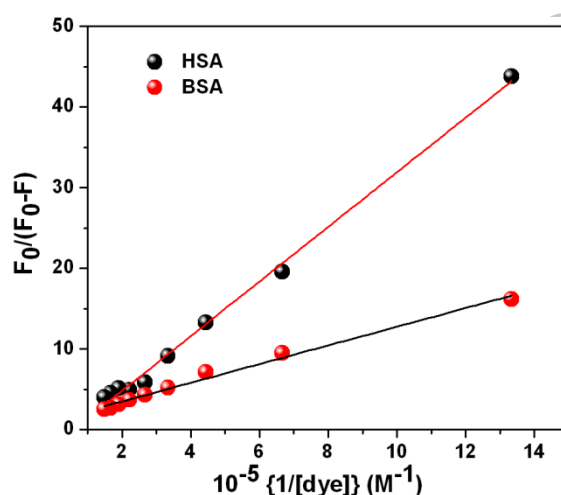


Fig. 6: Modified Stern-Volmer plot of dye-serum protein system

The value of  $K_a$  has been determined from intercept to slope ratio using this equation and found  $5.71 \times 10^4$  and  $7.47 \times 10^4$  for HSA and BSA respectively. From the above result it is clear that the dye forms moderately strong complex with the proteins. The results obtained in our present study are consistent with the previous literature reports (Sharma et. al., 2014; Tian et. al., 2004).

### 3.2.4. Determination of stoichiometry of dye-protein complex

Spectral data from the emission titration experiment has been utilized to calculate the stoichiometry of dye-protein complex using the Benesi–Hildebrand equation [eq. 6] (Benesi et. al., 1949).

$$\frac{1}{F_0 - F} = \frac{1}{F_0 - F_1} + \frac{C^o}{(F_0 - F_1)K[Q]}$$

(6)

Where,  $F_0$  is the emission intensity of HSA/ BSA in the absence of dye,  $F$  is the corrected emission intensity of the serum proteins at intermediate concentration of the dye,  $F_1$  is the emission intensity of HSA/ BSA at infinite concentration of dye,  $K$  is the binding constant and  $Q$  is the quencher (dye).

From Fig. 7(a) and (b), it has been seen that the plots of  $1/[F_0 - F]$  versus  $1/[\text{dye}]$  show a fine linearity, thereby suggesting one-to-one interaction between dye and HSA/ BSA.

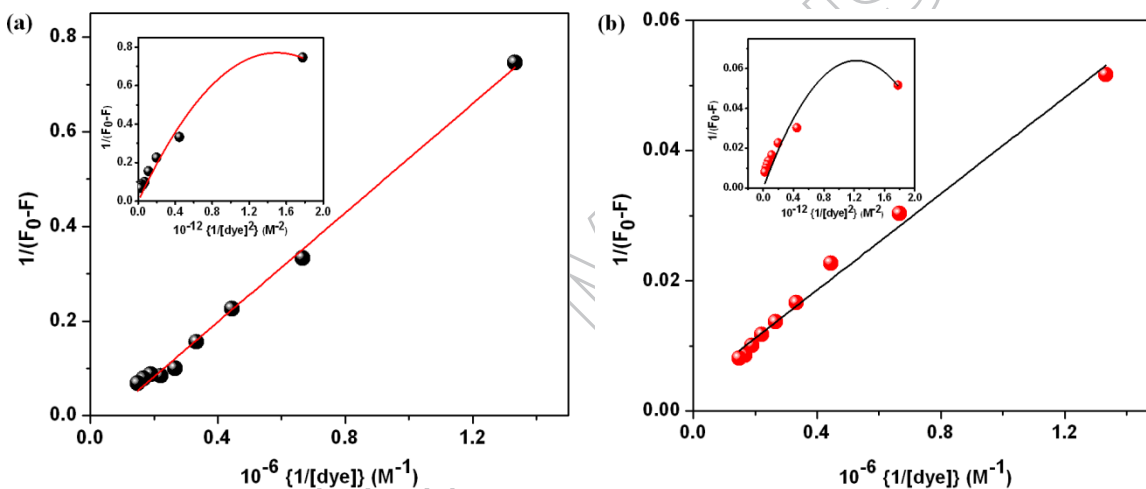


Fig. 7: Benesi-Hildebrand plot of  $1/[F_0 - F]$  versus  $1/[\text{dye}]$  for binding of dye with (a) HSA and (b) BSA. Inset shows the modified Benesi-Hildebrand plot of  $1/[F_0 - F]$  versus  $1/[\text{dye}]^2$  for HSA/ BSA-dye systems

It is broadly accepted that the linearity in Benesi-Hildebrand plot is indicative of 1:1 complexation (Samanta et. al., 2011). In our present study we have applied the modified Benesi-Hildebrand equation to validate the existence of 1:1 complexation and to exclude the possibility of 1:2 complex formations in dye-protein system. From the inset plots of Fig.7,  $1/(F_0-F)$  versus

$1/[\text{dye}]^2$  clearly shows a deviation from linearity indicating the nonexistence of 1:2 complexation (Samanta et. al., 2011).

Ostensibly, it is very much important at this stage to find the mechanistic interpretation of dye induced quenching of intrinsic fluorescence of the proteins. The two different quenching mechanism dynamic (collisional) and static can be distinguished by their differential dependence on temperature. Higher temperature leads to faster diffusion and greater extent of dynamic quenching but in case of static process reverse is true. In our present work occurrence of static quenching is proved from some experimental evidence but due to delve the presence of excited state complexation or dynamic quenching another important technique, time resolved fluorimetric analysis has been done.

### 3.2.5. Time resolved Fluorescence decay studies

Intrinsic Fluorescence life time decay measurement has become a promising tool for determining the conformational dynamics of the proteins and it is also very much sensitive to identify excited state interaction (Santhamani et. al., 2013). In our present study to gather clear information about dye-protein excited state complexation, time resolved fluorometric measurements have been done. The amendment of Trp life time upon regular addition of azo dye has been investigated and corresponding decay profiles of it has been displayed at Table 1.

Table 1(a): Fluorescence decay parameter of HSA as a function of added azo dye

Azo dye ( $\mu\text{M}$ )	$\tau_1(\text{ns})$	$A_1$	$\tau_2(\text{ns})$	$A_2$	$\langle\tau\rangle(\text{ns})$	$\chi^2$
0	3.33	0.3839	6.68	0.6161	5.39	1.05
4	3.06	0.4256	6.56	0.5744	5.08	1.03

8	2.95	0.4711	6.51	0.5289	4.83	1.02
12	3.09	0.5042	6.39	0.4958	4.73	1.05
16	2.82	0.5223	6.31	0.4777	4.50	1.01

Table 1(b): Fluorescence decay parameter of BSA as a function of added azo dye

Azo dye ( $\mu\text{M}$ )	$\tau_1$ (ns)	$A_1$	$\tau_2$ (ns)	$A_2$	$\langle\tau\rangle$ (ns)	$\chi^2$
0	3.0204	0.3069	6.3696	0.6931	5.34	1.02
4	2.3940	0.3980	6.0363	0.6020	4.58	1.06
8	2.0033	0.5565	5.8013	0.4435	3.69	1.02
12	1.6289	0.6213	5.5318	0.37875	3.11	1.04
16	1.58204	0.6825	5.3404	0.3175	2.77	0.99
20	1.5188	0.7300	5.0604	0.2700	2.61	1.05

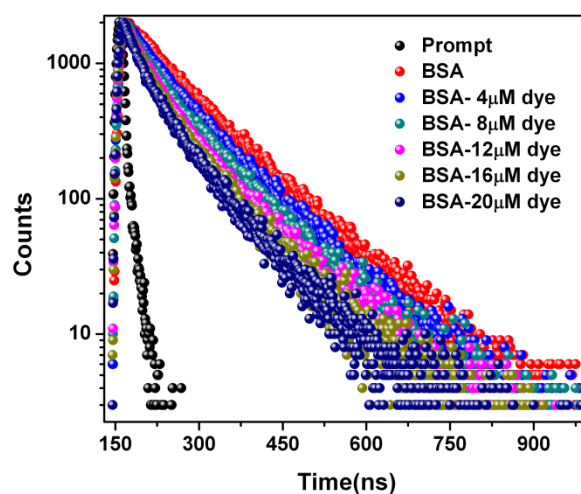
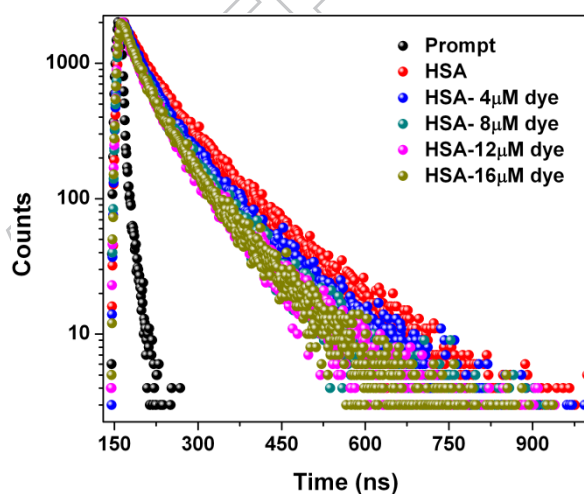


Fig. 8: Lifetime decay curves of serum proteins in the presence of various concentrations of dye

From the Fig. 8 it has been seen that the added dye decreases protein lifetime indicating excited state interaction between them. The Trp emission has been fitted to a bi-exponential decay, and the respective data have been summarized in Table 1(a) for HSA and Table 1(b) for BSA. As it is a non trivial task to assign the explicit mechanistic interpretation for the individual decay components within multi-exponential fluorescence decays in complex biological environments, we have taken an attempt to consider variation of the relative amplitudes of the two components of albumins upon gradual addition of dye (Berezin et. al., 2010; De et. al., 2013).

The decay profiles of both the proteins help us to conclude the presence of dynamic quenching upon action of quencher. The extent of dynamic fashion in the quenching mechanism of aforementioned dye-protein systems has been evaluated using the equation (Lakowicz, 2006)

$$\frac{\tau_0}{\tau} = 1 + K_D \frac{[Q]}{C^o} \quad (7)$$

Where  $\tau_0$  and  $\tau$  are the fluorescence lifetimes of the proteins in the absence and presence of the dye, respectively, and  $K_D$  is the dynamic quenching constant. The observation based on life time data and the plot  $\tau_0/\tau$  versus [dye] (Fig. S4) of dye-protein system, the  $K_D$  has been determined as  $1.18 \times 10^4$  and  $5.56 \times 10^4$  for HSA and BSA respectively. From the steady state and time resolved spectroscopy it is concluded that in our present contribution the dye quenches the emission intensity of the serum albumins by both static and dynamic fashion. In the mechanistic assay of the quenching process the contribution of static fashion has been determined using the following equation (Lakowicz, 2006)

$$\frac{\left[ \frac{F_0 - F}{F} \right] C^o}{[Q]} = (K_S + K_D) + K_S K_D \frac{[Q]}{C^o} \quad (8)$$

Using the slope of the plot  $[(F_0 - F)/F]/[Q]$  versus  $[Q]$  (Fig. S5),  $K_s$  have been calculated as  $2.15 \times 10^5$  and  $8.54 \times 10^4$  for HSA and BSA respectively. The results illustrate the greater amount of static quenching constant than that of dynamic quenching constant for both the proteins which indicates that the quenching mechanism is predominantly static rather than dynamic.

### 3.2.6. Binding constants and number of binding sites:

A quantitative assessment for the dye-protein binding interaction can be derived in terms of estimation of the binding constant ( $K_b$ ) and the free energy change ( $\Delta G$ ) for the interaction process. The binding constant plays a vital role because of the binding ability and subsequent influence of drugs on protein stability will govern the therapeutic efficacy of the drug to a large extent. For static quenching process when a small molecule binds independently to a set of equivalent sites on macromolecule, then the equilibrium between the free molecule and bound molecule is given by double-logarithmic equation (Lakowicz, 2006)

$$\log\left(\frac{F_0 - F}{F}\right) = \log(K_b) + n \log\left(\frac{[Q]}{C^o}\right) \quad (9)$$

.Where  $K_b$  is the binding constant and  $n$  is the number of binding sites. According to the equation the values of  $K_b$  and  $n$  can be obtained from the intercept and slope of the above equation. The results for the present investigation at various temperatures have been summarized in Table 2 and the representative plots of  $\log [(F_0 - F)/F]$  versus  $\log ([dye]/C^o)$  have been displayed in Fig.

9.

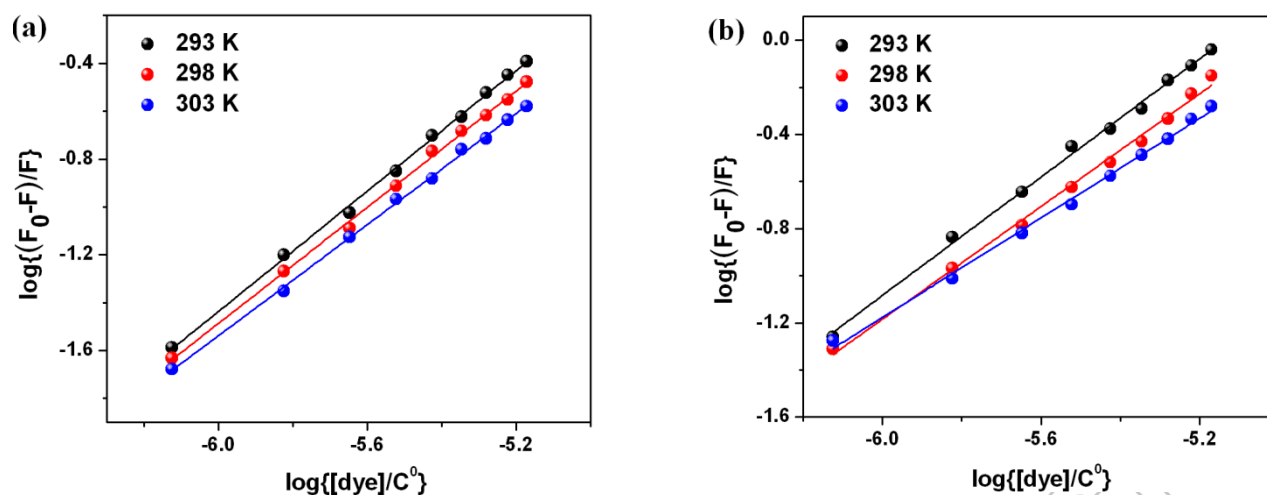


Fig. 9: Plots of  $\log [(F_0-F)/F]$  versus  $\log([dye]/C^0)$  at different temperatures representing effect of temperature on binding of dye with (a) HSA and (b) BSA, pH 7.4

Table 2: Summary of the Binding Parameters for the dye–protein interaction from Fluorescence Quenching Data for HSA and BSA respectively

Temperature (K)	HSA		BSA	
	$10^{-6} \times K_b$	$n$	$10^{-6} \times K_b$	$n$
293	1.28	1.25	2.82	1.26
298	0.61	1.21	0.98	1.19
303	0.26	1.15	0.15	1.05

From the data collected in Table 2 we see that our results evidently demonstrate that the dye–protein binding strength becomes weak with increasing temperature which appears to reinforce the postulate of a predominant static quenching mechanism rather than dynamic process in the presently studied system in confirmation to the aforementioned discussion.

### 3.2.7. Thermodynamic Parameters and Nature of the Binding Forces

The knowledge of the actual binding forces originating from the drug–protein interaction process is of immense importance in protein chemistry, and deciphering of the thermodynamics of the

interaction process provides a profound acumen to the mechanistic aspects involved. Usually, the interaction forces between drugs and biomolecules may be assorted including electrostatic, hydrogen bonding, van der Waals interaction, hydrophobic, and steric contacts within the binding site, and so forth (Paul et. al., 2011; Klotz et. al., 1973; Ross et. al., 1981). The sign and magnitudes of thermodynamic parameters are very much important to insight the principle binding forces (Klotz et. al., 1973; Ross et. al., 1981).

If we consider that there is no significant variation of the enthalpy change ( $\Delta H$ ) within the range of temperature studied, both the enthalpy change ( $\Delta H$ ) and the entropy change ( $\Delta S$ ) can be evaluated from van't Hoff's equation: (Klotz et. al., 1973)

$$\ln K = -\frac{\Delta H}{R} \times \frac{1}{T} + \frac{\Delta S}{R} \quad (10)$$

Here, R is the universal gas constant, and T is the temperature in kelvin. The free energy change ( $\Delta G$ ) of the process is then evaluated from the following relationship:

$$\Delta G = \Delta H - T\Delta S \quad (11)$$

The thermodynamic parameters have been calculated from the van't Hoff plot ( $\ln K$  vs.  $1/T$ ) which is displayed in (Fig. S6). In protein chemistry the various individual kinds of interaction are characterized with the thermodynamic parameters such as: (Paul et. al., 2014)

- (i)  $\Delta H > 0$ ,  $\Delta S > 0$  correspond to hydrophobic forces;
- (ii)  $\Delta H < 0$ ,  $\Delta S < 0$  correspond to van der Waals interaction, hydrogen-bond formation;
- (iii)  $\Delta H < 0$ ,  $\Delta S > 0$  correspond to electrostatic/ionic interactions.

The derived thermodynamic parameters suggest that dye-protein interaction is enthalpically favorable (-117.6 and -213.2 kJ mol<sup>-1</sup> for HSA and BSA respectively and both are < 0) but

entropically not favorable ( $-284.2$  and  $-603.8$  J mol<sup>-1</sup> K<sup>-1</sup> for HSA and BSA respectively and both are  $< 0$ ). With this we also get that the overall negative Gibbs free energy change ( $-22.9$  and  $-33.5$  kJ mol<sup>-1</sup> for HSA and BSA respectively) implies the spontaneity of the binding interaction. The negative entropy and enthalpy change signifies presence of van der Waals interaction or hydrogen bond formation between dye and serum proteins.

### **3.3. Effect of ionic strength on dye-protein interaction**

From the thermodynamic parameters it is clear that the binding interaction of azo dye with serum proteins does not involve electrostatic interaction in our present study but to ensure this, a strong electrolyte NaCl has been added to the dye-protein system. In order to study the effect of ionic strength on the binding interaction, the NaCl concentration has been varied from 0 to 50 mM. No considerable change in binding constant has been observed in the presence of high concentration of NaCl (figure not shown). The incident clearly indicates that electrostatic forces have no significant contribution in the drug-protein interaction process. Thus, van der Waals interaction or H-bond formation is major contributing binding force for dye-protein system.

### **3.4. Fluorescence Resonance Energy Transfer from protein to azo dye**

Fluorescence Resonance Energy Transfer (FRET) is a distance dependent interaction between the different electronic excited states of molecules in which excitation energy is transferred from donor molecule to acceptor molecule without emission of a photon from the former molecular system (Förster, 1959). When the emission spectrum of a fluorophore (protein) overlaps with the absorption spectrum of acceptor (ligand) then FRET occurs. The spectral overlap between the UV absorption spectrum of dye and the fluorescence emission spectrum of HSA has been displayed in the Fig. 10. Similar spectral overlap has been also observed in case of BSA also

(spectra not shown).

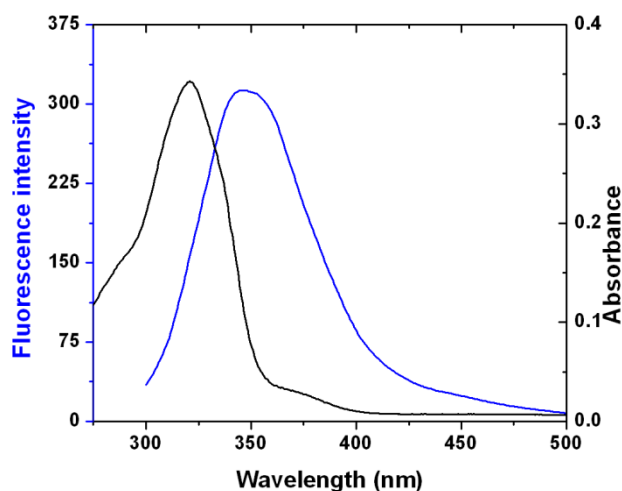


Fig. 10: Spectral overlap of UV-Vis absorption spectrum of synthesized dye with the fluorescence emission spectrum of HSA,  $[HSA] = [dye] = 5.0 \mu M$ ,  $T = 298 K$ .

The degree of energy transfer depends on the distance between donor and acceptor and extent of overlap. According to Förster's nonradiative energy transfer theory, the energy transfer efficiency ( $E$ ) is defined by the following equation:

$$E = 1 - \frac{F}{F_0} = \frac{R_0^6}{R_0^6 + r^6} \quad (12)$$

Where  $F$  and  $F_0$  are fluorescence intensities of serum proteins in presence and absence of dye,  $r$  is the distance between acceptor and donor, and  $R_0$  is the critical energy transfer distance when transfer efficiency is 50%. The value of  $R_0$  has been evaluated using the equation below:

$$R_0 = 8.8 \times 10^{-25} \kappa^2 N^{-4} \Phi J \quad (13)$$

Where  $\kappa^2$  is spatial orientation factor of the dipole,  $N$  is refractive index of the medium,  $\Phi$  is the fluorescence quantum yield of the donor, and  $J$  is the overlap integral of the fluorescence emission spectrum of donor and absorption. Now  $J$  is given by the following equation:

$$J = \frac{\sum F(\lambda) \varepsilon(\lambda) \lambda^4 \Delta\lambda}{\sum F(\lambda) \Delta\lambda} \quad (14)$$

Where  $F(\lambda)$  is the fluorescence intensity of the fluorescent donor of wavelength  $\lambda$ ,  $\varepsilon(\lambda)$  is the molar absorption coefficient of the acceptor at wavelength  $\lambda$  (Tian et.al., 2010). In our present contribution  $\kappa^2 = 2/3$ ,  $N = 1.336$  and  $1.36$ ,  $\Phi = 0.118$  and  $0.15$  for HSA and BSA respectively (Cui et. al., 2003; Li et. al., 2007).

Utilizing above equations the value of overlap integral ( $J$ ),  $R_0$ ,  $E$ , and  $r$  have been calculated and found to be  $3.07 \times 10^{-14} \text{ cm}^3 \text{ L mol}^{-1}$ ,  $2.96 \text{ nm}$ ,  $0.17$  and  $3.85 \text{ nm}$  for HSA and  $2.84 \times 10^{-14} \text{ cm}^3 \text{ L mol}^{-1}$ ,  $4.42 \text{ nm}$ ,  $0.36$  and  $4.84 \text{ nm}$  for BSA respectively. For energy transfer process an essential criterion is that the distance between donor and acceptor must be within 2–8 nm (Förster, 1959). This criterion is satisfied in the present study and hence quenching of protein (HSA and BSA) fluorescence in the presence of the dye is attributed to energy transfer.

### 3.5. Conformation Investigation: Circular Dichroism (CD) Spectral Study

Circular dichroism (CD) spectroscopy has long been recognized as a powerful technique to investigate the conformational alteration of a variety of bimolecular systems including proteins upon action of different drug molecules (Sreerama et. al., 2000). Fig. 11 reveals far UV circular dichroism spectra of proteins in absence and presence of different dye concentrations.

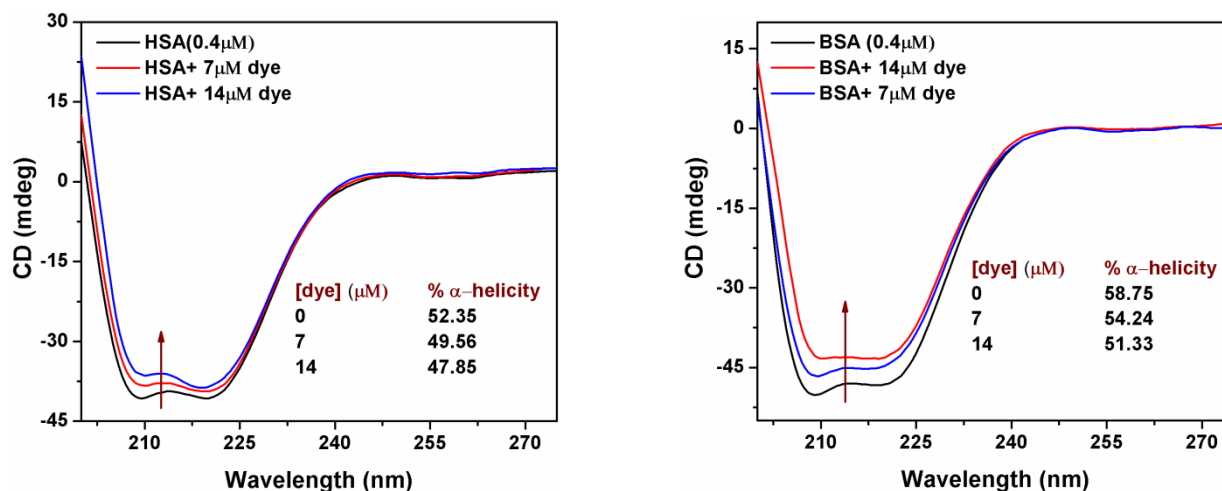


Fig. 11: CD spectra of HSA and BSA in absence and presence of dye

It is noteworthy here that the dye does not give any CD signal within 200 and 280 nm. So, only serum proteins give the CD signals exclusively, shown in Fig. 11. The CD spectra of the serum proteins are characterized by two negative bands at 208 and 222 nm due to  $\pi \rightarrow \pi^*$  and  $n \rightarrow \pi^*$  transition in the peptide bonds of  $\alpha$ -helix respectively (Yang et. al., 2002). As is evident from the figure, increasing dye concentration leads to decrease of CD signal of the far-UV CD spectral profile of serum albumins representing the conformational change in proteins secondary structure upon action of the dye.

### 3.6. Dye-Induced Modulation in the Functionality of serum albumins: Esterase-like Activity

In addition to the well-known ligand binding capacity, serum proteins have remarkable promiscuous catalytic activities toward various organic molecules, including esters, amides, phosphates etc (Kim et. al., 2013; Paul et. al., 2013). Being conscious about the considerable impact of the binding of azo dye on the native conformation of serum proteins, it is significant to

highlight the issue of ligand-protein interaction, as per its biological consequences. HSA has significantly greater esterase-like activity than BSA. The esterase-like activity of the proteins has been assessed by the well-established technique of monitoring the absorbance of p-nitrophenol ( $\lambda_{\text{abs}} = 400 \text{ nm}$ ,  $\epsilon = 17,700 \text{ M}^{-1} \text{ cm}^{-1}$ ) as produced by the action of proteins on p-nitrophenyl acetate.

The activity of serum proteins under various experimental conditions has been estimated following the definition that one unit of activity refers to the amount of the enzyme (protein) required to liberate  $1.0 \mu\text{M}$  p-nitrophenol per minute at  $37 \text{ }^\circ\text{C}$ . From site directed mutagenesis studies it has been observed that Arg 410 and Tyr 411 of HSA at subdomain III A are essential for esterase activity (Ascenzi et. al., 2012). In this article, Fig 12(a) portrays that our ligand do not have any significant effect on esterase activity of HSA. This finding reveals that our synthesized dye don't assemble at subdomain IIIA. Exact binding location can be predicted from molecular docking studies as will be discussed in the following section.

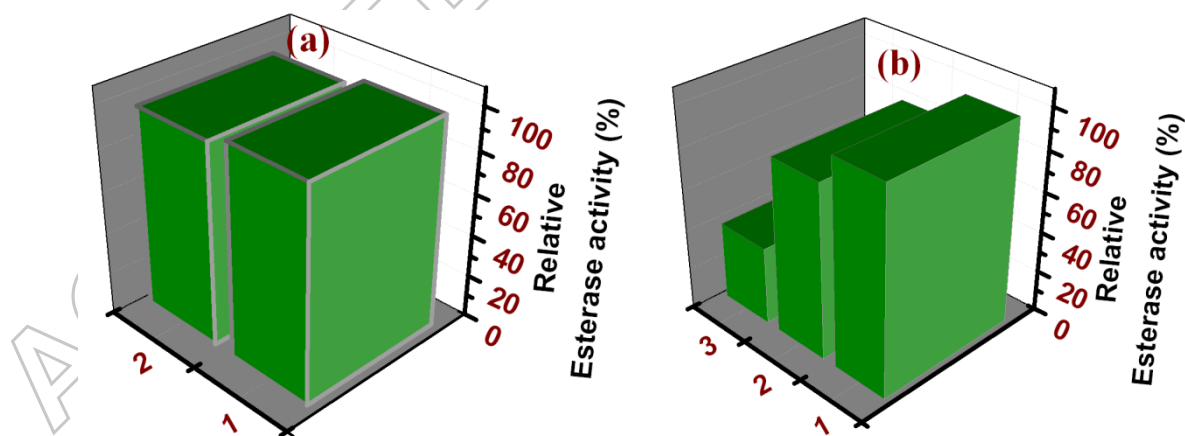


Fig. 12: (a) Dye-induced modulation of the esterase-like activity profile of HSA ( $[\text{dye}] = (1) 0$ ,

(2) 50  $\mu\text{M}$ ). (b) BSA ([dye] = (1) 0, (2) 25, (3) 50  $\mu\text{M}$ )

On the other hand in case of BSA, Fig.12 (b) depicts a representative profile for the effect of the dye on the esterase activity of BSA. According to experimental synopsis, binding with dye is associated with an appreciable reduction in the esterase activity of BSA, which exposes remarkable breakdown of the native protein structure upon interaction with the dye.

### 3.7. Cytotoxicity and antiviral activity studies

In-vitro cytotoxic activity of our synthesized compound against vero cell line has been tested using MTT assay. As illustrated in Fig. 13, cytotoxicity of the tested compound against the cell increases with increasing its concentration. The value of  $\text{IC}_{50}$  has also been calculated from the MTT assay results.  $\text{IC}_{50}$  is nothing but treatment of minimum concentration of compound where 50 % of cell population is survived. In our present contribution the value obtained is almost 100  $\mu\text{g mL}^{-1}$ . Fig. 13: displays the percentage of cell viability against concentration of synthesized dye. These results indicate that the dye has huge potential in vitro as well as in vivo applications.

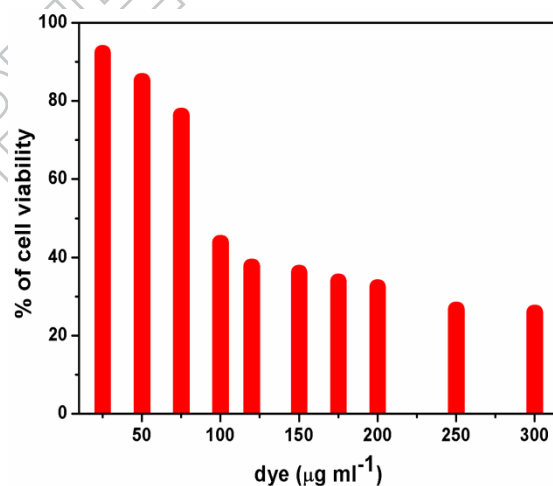


Fig. 13: Cell viability data (MTT assay) of the dye

An efficacy study has been conducted to determine whether the synthesized dye would have a

therapeutic benefit against HSV-1F virus infection on vero cell. Tolerability studies have been performed with injections of dye on virus affected cell at levels of upto  $160 \mu\text{g mL}^{-1}$ . Fig. 14 show that the dye can inhibit virus in a dose dependent manner. From the result obtained, maximum inhibition occurs at  $80 \mu\text{g mL}^{-1}$  of dye.

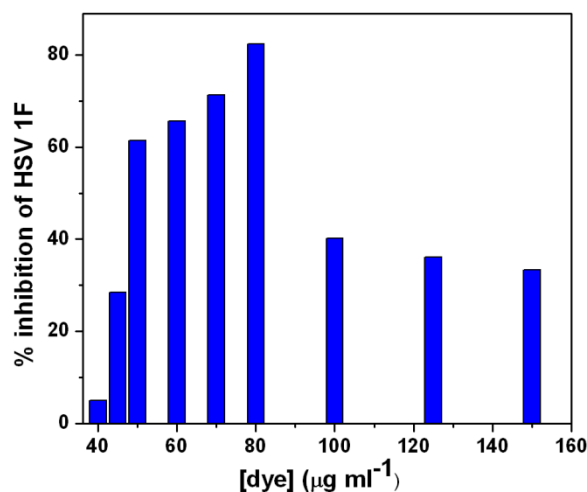


Fig. 14: % inhibition of HSV-1F virus upon action of dye

### 3.8. Molecular Docking analysis

In modern era, molecular docking study plays an exigent role in revealing the mode of binding of a small molecule relative to a macromolecular architecture like protein, DNA etc. Recently, the application of docking simulation in predicting the binding of surfactant and dye to macromolecules has been encountered by our research group (Dasmandal et. al., 2015; Rudra et. al., 2016). In this present work, molecular modeling has been accomplished to explore the binding regions offered by BSA/HSA to our synthesized azo dye investigated. In order to corroborate the experimental results, 25 possible docked conformations each of the BSA-dye and HSA-dye complex have been modeled by AutoDock program (as mentioned in the method

section), out of which one conformation from each pair with the highest negative binding energy have been considered to be the best ranked results, and shown as well in Fig. 15.

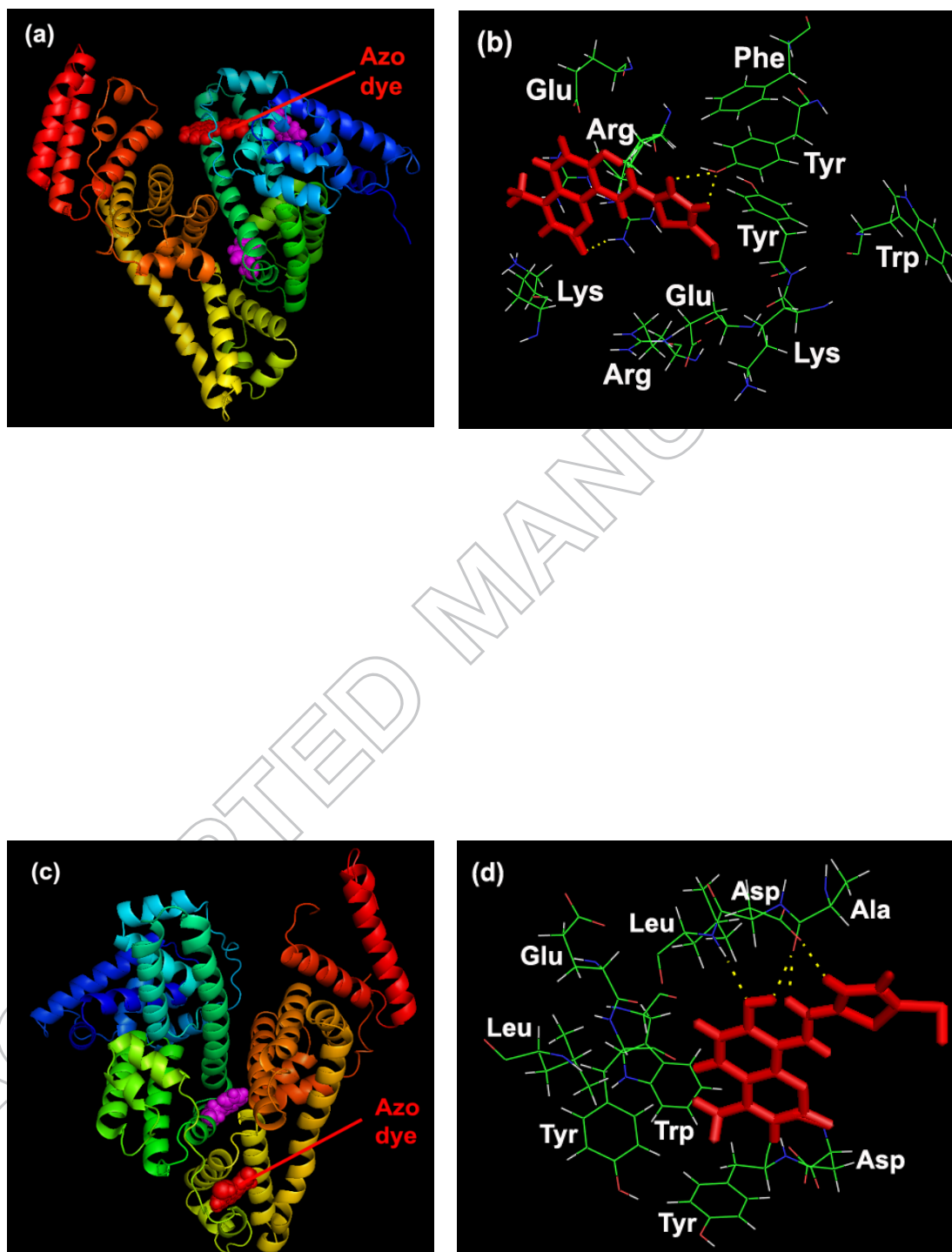


Fig.15: (a) & (c) are the lowest energy binding modes of azo dye to BSA and HSA respectively.

Secondary structure of BSA and HSA are displayed by ribbon and tube with magenta colored Trp residues (space ball), and azo dye is displayed by space ball and colored in dark red. (b) & (d) are close-up view of binding site of dye on BSA and HSA corresponding to (a) & (c) where dye has been shown by stick model (red colored) and the selected amino acid residues are shown

by line model with color variants as:



Possible H-bonding interactions are shown in yellow dotted line.

From the docking study, binding energy of the most favorable docked form corresponding to BSA-dye and HSA-dye complex has been evaluated as  $-18.9$  and  $-16.8$   $\text{kJ mol}^{-1}$  respectively. However, the standard free energy changes ( $\Delta G^\circ$ ) for binding of dye to BSA and HSA calculated experimentally *i.e.*,  $-33.5$  and  $-22.9$   $\text{kJ mol}^{-1}$  respectively, is somewhat different from that computed theoretically. This unavoidable difference in the energy value of the respective pair is due to the X-ray structure of BSA/HSA extracted from crystal is significantly different from that in the aqueous system used in the present study. This in turn offers different microenvironment to azo dye to bind with BSA/HSA.

A close-up view of the docked form corresponding to BSA-dye complex has been shown in Fig. 15 (b) which reveals that dye binds to BSA in sub-domain IB. In this region, dye is surrounded by a number of amino acid residues such as Phe-164, Glu-182, Tyr-137, Tyr-160, Trp-134, Lys-136, Arg-144, Glu-140, Lys-114, Arg-185. Docking study reveals the possibilities of H-bonding interactions of the dye with Tyr-160 and Arg-185 amino acid residues of BSA. Thus both hydrophobic and H-bonding interactions are operating in BSA-dye system as obtained from thermodynamic analysis in experimental section and the interaction results considerable changes in spectroscopic properties of BSA.

The close-up view of docked form corresponding to HSA-dye complex has been shown in Fig. 15(d). The Fig. 15(d) reveals that dye binds to HSA in sub-domain IIA. In this region, dye is found to be enclosed by amino acid residues *viz*, Glu-333, Leu-305, Trp-214, Tyr-334, Tyr-341, Asp-340, Leu-302, Asp-301 and Ala-300. Here H-bonding of dye with Leu-302, Asp-301 and Ala-300 of HSA has been observed. From theoretical point of view, the dye interacts with human serum protein may be through H-bonding as obtained from thermodynamic analysis in experimental section.

#### 4. Conclusion

The results of integrated experimental and theoretical studies explain the binding interaction of a synthesized dye with two serum proteins, under physiological conditions. The binding parameters for dye-protein system have been systematically derived from the emission titration experiments. Life time and temperature dependent fluorimetric analysis reveals the actual mechanistic assay of the dye-protein complexation which includes presence of both static and dynamic nature of quenching. An extensive thermodynamic analysis of the dye-protein binding phenomenon suggests the pivotal role of van der Waals interaction or hydrogen bond formation in the process, and the absence of ionic interaction is found to be supported by observing the binding phenomena in presence of strong electrolyte NaCl. The absorption and CD spectral studies divulge that the dye causes some micro environmental and conformational changes in the secondary structure of SAs. The extent of energy transfer between donor (protein) and acceptor (dye) has been measured by calculating distances between them as 3.85 and 4.84 nm for HSA and BSA respectively using the idea of FRET. The dye induced modulation of protein functionality produces a comprehensive accepting of the fact that the proteins exhibit maximum

efficiency towards esterase activity in its native conformation. No significant alteration of esterase activity in case of HSA but remarkable effect has been observed in case of BSA. The AutoDock-based docking simulation study recognizes the exact location of dye on protein macromolecules as subdomain IB for BSA and subdomain IIA for HSA respectively. With this protein binding capacity dye also exhibits significant cytotoxicity towards Vero cell and anti viral activity on **HSV-1F** affected Vero cell. These findings present detail insight to understand the binding properties of dye to SAs, which may be beneficial for industrial and pharmaceutical applications in future.

## Acknowledgement

SR is grateful to the Department of Science & Technology (DST), New Delhi, for INSPIRE fellowship.

## References

Akbaya, N., Topkayab, D., Ergün, Y., Alp, S., & Gök, E. (2010). Fluorescence Study on the Interaction of Bovine Serum Albumin with Two Coumarin Derivatives, *J. Anal. Chem.*, 65, 382–387. doi: 10.1134/S1061934810040088.

Amin, K. A., Hameid, H. A., & Abd Elsttar, A. H. (2010). Effect of food azo dyes tartrazine and carmoisine on biochemical parameters related to renal, hepatic function and oxidative stress biomarkers in young male rats. *Food Chem. Toxicol.*, 48, 2994–2999.  
<https://doi.org/10.1016/j.fct.2010.07.039>.

Andrade, S. M., & Costa, S. M. B. (2002). Spectroscopic studies on the interaction of a water soluble porphyrin and two drug carrier proteins. *Biophys. J*, *82*, 1607–1619. doi:10.1016/S0006-3495(02)75512-4.

Arumugam, S. S., Subramanian, N., & Malaichamy, I. (2016). New insights into the dimerization and site-specific cooperative interaction of Azure B with model transport proteins by spectroscopic and computational studies. *J. Photochem. Photobiol. B, Biol.*, *164*, 212–225. doi: 10.1016/j.jphotobiol.2016.09.011.

Ascenzi, P., Gioia, M., Fanali, G., Coletta, M., & Fasano, M. (2012). Pseudo-enzymatic hydrolysis of 4-nitrophenyl acetate by human serum albumin: pH-dependence of rates of individual steps. *Biochem. Biophys. Res. Commun*, *424*, 451–455. <https://doi.org/10.1016/j.bbrc.2012.06.131>.

Bayraktutan, T., & Onganer, Y. (2017). Spectral-luminescent study of coumarin 35 as fluorescent “light-up” probe for BSA and DNA monitoring. *Dyes Pigm*, *142*, 62-68. doi:10.1016/j.dyepig.2017.03.019.

Benesi, H. A., & Hildebrand, J. H. (1949). A spectrophotometric investigation of the interaction of iodine with aromatic hydrocarbons. *J. Am. Chem. Soc.*, *71*, 2703–2707. doi:10.1021/ja01176a030.

Berezin, M. Y., & Achilefu, S. (2010). Fluorescence Lifetime Measurements and Biological

Imaging. *Chem. Rev.*, *110*, 2641–2684. doi:10.1021/cr900343z.

Carter, D. C., & Ho, J. X. (1994). Structure of Serum-Albumin. *Adv. Protein Chem*, *45*, 153–203. [https://doi.org/10.1016/S0065-3233\(08\)60640-3](https://doi.org/10.1016/S0065-3233(08)60640-3).

Chen, J., Liu, W., Zhou, B., Niu, G., Zhang, H., Wu, J.,... Wang, P. (2013). Coumarin- and rhodamine-fused deep red fluorescent dyes: synthesis, photophysical properties, and bioimaging in vitro. *J Org Chem*, *78*, 6121–6130. doi:10.1021/jo400783x.

Chowdhury G. (1996). Human health perspectives on environmental exposure to benzidine: A review. *Chemosphere*, *32*, 267–291.

Christie, R. M., Morgan, K. M., & Islam, M. S. (2008). Molecular design and synthesis of N-arylsulfonated coumarin fluorescent dyes and their application to textiles. *Dyes Pigm*, *76*, 741–747.

Cui, F. L., Fan, J., Ma, D. L., Liu, M. C., Chen, X. G., & Hu, Z. D. (2003). A Study of the interaction between a new reagent and serum albumin by fluorescence spectroscopy. *Anal. Lett*, *36*, 2151–2166. <https://dx.doi.org/10.1081/AL-120023708>.

Dan, A., Chakraborty, I., Ghosh, S., & Moulik, S. P. (2007). Interfacial and Bulk Behavior of Sodium Dodecyl Sulfate in Isopropanol-Water and in Isopropanol-Poly(vinylpyrrolidone)-Water Media. *Langmuir*, *23*, 7531–7538. doi:10.1021/la700557m.

Dasmandal, S., Kundu, A., Rudra, S., & Mahapatra, A. (2015). Binding Interaction of an Anionic

Amino Acid Surfactant with Bovine Serum Albumin: Physicochemical and Spectroscopic investigations combined with Molecular Docking Study. *RSC Adv.*, 5 79107-79118.

doi:10.1039/C5RA17254C.

De, D., & Datta, A. (2013). Unique Effects of Aerosol OT Lamellar Structures on the Dynamics of Guest Molecules. *Langmuir*, 29, 7709–7714. doi: 10.1021/la401564b.

Efink, M. R., & Ghiron, C. A. (1976). Exposure of tryptophanyl residues in proteins Quantitative determination by fluorescence quenching studies. *Biochemistry*, 15, 672–680.

doi:10.1021/bi00648a035.

Förster T. (1959). 10th Spiers Memorial Lecture. Transfer mechanisms of electronic excitation. *Discuss. Faraday Soc.*, 27, 7–17.

Kelly, S. M., Jess, T. J., & Price, N. C. (2005). How to study proteins by circular dichroism. *Biochim. Biophys. Acta*, 1751, 119–139. doi:10.1016/j.bbapap.2005.06.005.

Khan, A. Y., Hossain, M., & Kumar, G. S. (2012). Investigations on the interaction of the phototoxic alkaloid coralyne with serum albumins. *Chemosphere*, 87, 775–781. doi: 10.1016/j.chemosphere.2011.12.079.

Kim, S. J., Rhee, H. W., Park, H. J., Kim, H. Y., Kim, H. S., & Hong, J. I. (2013). Fluorescent probes designed for detecting human serum albumin on the basis of its pseudo-esterase activity.

*Bioorg. Med. Chem. Lett*, 23, 2093–2097. <https://doi.org/10.1016/j.bmcl.2013.01.124>.

Klotz, I. M., (1973). Physiochemical aspects of drug-protein interactions: A general perspective. *Ann. N. Y. Acad. Sci.*, 226, 18–35. doi:10.1111/j.1749-6632.1973.tb20465.x.

Koh, W., & Sham, L. J. (1965). Self-consistent Equations Including Exchange and Correlation Effects. *Phys Rev*, 140, 1133-1138. doi: <https://doi.org/10.1103/PhysRev.140.A1133>.

Lakowicz, J. R. (Ed. 3<sup>rd</sup>) (2006). Principles of Fluorescence Spectroscopy, USA: Springer.

Lano, W. L. D. (2004). PyMOL Molecular Graphics System. [De Lano Scientific, San Carlos, CA]. Retrieved from <http://pymol.sourceforge.net/>.

Li, D. J., Zhu, J. F., & Jin, J. (2007). Spectrophotometric studies on the interaction between nevadensin and lysozyme. *J. Photochem. Photobiol. A*, 189, 114–120.

doi:10.1016/j.jphotochem.2007.01.017.

Lou, Y. Y., Zhou, K. L., Pan, D. Q., Shen, J. L., & Shi, J. H. (2017). Spectroscopic and molecular docking approaches for investigating conformation and binding characteristics of clonazepam with bovine serum albumin (BSA). *J. Photochem. Photobiol. B, Biol*, 167, 158–167.

<https://doi.org/10.1016/j.jphotoboil.2016.12.029>.

Medvedev, Z. A., Crowne, H. M., & Medvedeva M. N. (1988). Age related variations of hepatocarcinogenic effect of azo dye (30- MDAB) as liked to the level of hepatocyte polyploidization. *Mech Ageing Dev*, 46, 159–174.

Mohamadi, M., Hassankhani, A., Ebrahimipour, S. Y., & Torkzadeh-Mahani, M. (2017). In vitro and in silico studies of the interaction of three tetrazoloquinazoline derivatives with DNA and BSA and their cytotoxicity activities against MCF-7, HT-29 and DPSC cell lines. *Int. J. Biol. Macromolec.*, *94*, 85–95. <https://doi.org/10.1016/j.ijbiomac.2016.09.113>.

Morris, G. M., Goodsell, D. S., Halliday, R. S., Huey, R., Hart, W. E., Belew, R. K., & Olson, A. J. (1998). Automated Docking Using a Lamarckian Genetic Algorithm and Empirical Binding Free Energy Function. *J. Comput. Chem.*, *19*, 1639–1662. doi: 10.1002/(SICI)1096-987X(19981115)19:14<1639::AID-JCC10>3.0.CO;2-B.

Mosmann, T. (1983). Rapid colorimetric assay for cellular growth and survival: Application to proliferation and cytotoxicity assays. *J. Immunol. Methods*, *65*, 55–63. [https://doi.org/10.1016/0022-1759\(83\)90303-4](https://doi.org/10.1016/0022-1759(83)90303-4).

Pan, X., Qin, P., Liu, R., & Wang, J. (2011). Characterizing the interaction between tartrazine and two serum albumins by a hybrid spectroscopic approach. *J. Agric. Food Chem.*, *59*, 6650–6656. doi: 10.1021/jf200907x.

Paul, B. K., & Guchhait, N. (2011). Exploring the strength, mode, dynamics, and kinetics of binding interaction of a cationic biological photosensitizer with DNA: Implication on dissociation of the drug- DNA complex via detergent sequestration. *J. Phys. Chem. B*, *115*, 11938-11949. doi: 10.1021/jp206589e.

Paul, B. K., Ray, D., & Guchhait, N. (2013). Unraveling the binding interaction and kinetics of a prospective anti-HIV drug with a model transport protein: results and challenges. *Phys. Chem. Chem. Phys.*, *15*, 1275–1287. doi: 10.1039/c2cp42539d.

Paul, B. K., Ghosh, N., & Mukherjee, S. (2014). Binding Interaction of a Prospective Chemotherapeutic Antibacterial Drug with  $\beta$ -Lactoglobulin: Results and Challenges. *Langmuir*, *30*, 5921–5929. doi: 10.1021/la501252x.

Peters, T. (1985). *Advances in Protein Chemistry*. New York: Academic Press.

Peters, T., & Putman, F.W. (1975). *The Plasma Proteins*. Academic Press (pp. 133–181).

Popiolek, Ł., Biernasiuk, A., & Malm, A. (2015). New 5-substituted-1,3,4-thiadiazole-2(3H)-thione Derivatives: Synthesis and Their In vitro Antimicrobial Properties. *J. Am. Chem. Soc.*, *6*, 136-143. doi: 10.9734/ACSj/2015/16229.

Qin, M., Yin, T. & Shen, W. (2016). The Interaction Between Crystal Violet and Bovine Serum Albumin: Spectroscopic and Molecular Docking Investigations. *J Dispers Sci Technol.*, *37*, 1623-1629.

Ratna, & Padhi, B. S. (2012). Pollution due to synthetic dyes toxicity & carcinogenicity studies and remediation. *Int. J. Environ. Sci*, *3*, 940–955. doi: 10.6088/ijes.2012030133002.

Ross, P. D., & Subramanian, S. (1981). Thermodynamics of protein association reactions: Forces contributing to stability. *Biochemistry*, *20*, 3096–3102. doi: 10.1021/bi00514a017 and references

therein.

Roy, A., Seal P., Sikdar, J., Banerjee S. & Haldar, R. (2017). Underlying molecular interaction of bovine serum albumin and linezolid: A biophysical outlook. *J. Biomol. Struct. Dyn.*, 1-11, <http://dx.doi.org/10.1080/07391102.2017.1278721>.

Rudra, S., Dasmandal, S., Patra, C., Kundu, A., & Mahapatra, A. (2016). Binding affinities of Schiff base Fe(II) complex with BSA and calf-thymus DNA : Spectroscopic investigations and molecular docking analysis, *Spectrochim. Acta Mol. Biomol. Spectrosc*, 166, 84–94. doi: 10.1016/j.saa.2016.04.050.

Samanta, A., Paul, B. K., & Guchhait N. (2011). Spectroscopic probe analysis for exploring probe–protein interaction: a mapping of native, unfolding and refolding of protein bovine serum albumin by extrinsic fluorescence probe. *Biophys. Chem.*, 156, 128–139. <https://doi.org/10.1016/j.bpc.2011.03.008>.

Santhamani, N., & Sambandam, A. (2013), Binding of serum albumins with bioactive substances – nanoparticles to drugs. *J Photochem Photobiol C*, 14, 53–71. doi: 10.1016/j.jphotochemrev.2012.09.001.

Sharma, A. S., Anandhakumar, S., & Ilanchelian, M., (2014). A Combined spectroscopic and molecular docking study on site selective binding interaction of Toluidine blue O with Human

and Bovine serum albumins. *Lumin J.*, *151*, 206–218. doi: 10.1016/j.jlumin.2014.02.009.

Sreerama, N., & Woody, R. W. (2000). Estimation of Protein Secondary Structure from Circular Dichroism Spectra: Comparison of CONTIN, SELCON, and CDSSTR Methods with an Expanded Reference Set. *Anal. Biochem.*, *287*, 252–260. doi: 10.1006/abio.2000.4880.

Sudlow; G., Birkett, D. J., & Wade, D. N. (1975). The characterization of two specific drug binding sites on human serum albumin. *Mol. Pharmacol.*, *11*, 824–832.

Tian, J., Liu, J., He, W., Hu, Z., Yao, X., & Chen, X. (2004). Probing the Binding of Scutellarin to Human Serum Albumin by Circular Dichroism Fluorescence Spectroscopy, FTIR, and Molecular Modeling Method. *Biomacromolecules*, *5*, 1956–1961. doi: 10.1021/bm049668m.

Tian, F. F., Jiang, F. L., Han, X. L., Xiang, C., Ge, Y. S., Li, J. H., ... Liu, Y. (2010). Synthesis of a novel hydrazone derivative and biophysical studies of its interactions with bovine serum albumin by spectroscopic, electrochemical, and molecular docking methods. *J. Phys. Chem. B*, *114*, 14842–14853. doi: 10.1021/jp105766n.

Vaarla, K., Kesharwani, R. K., Santosh, K., Vedula, R. R., Kotamraju, S., & Toopurani, M. K. (2015). Synthesis, biological activity evaluation and molecular docking studies of novel coumarin substituted thiazolyl-3-aryl-pyrazole-4- carbaldehydes. *Bioorg. Med. Chem. Lett.*, *25*, 5797–5803. doi: 10.1016/j.bmcl.2015.10.042.

Xu, T., Guo, X., Zhang, L., Pan, F., Lv, J., Zhang, Y., & Jin, H. (2012). Multiple spectroscopic studies on the interaction between olaquinox, a feed additive, and bovine serum albumin. *Food Chem. Toxicol*, *50*, 2540–2546. <http://dx.doi.org/10.1016/j.fct.2012.04.007>.

Yang, P., & Gao, F. (2002) (pp. 349) *The Principle of Bioinorganic Chemistry*, Beijing, China: Science Press.

Zhao, X., Liu, R., Chi, Z., Teng, Y., & Qin, P. (2010). New insights into the behavior of bovine serum albumin adsorbed onto carbon nanotubes: comprehensive spectroscopic studies. *J. Phys. Chem. B*, *114*, 5625–5631. doi: 10.1021/jp100903x.

ACCEPTED MANUSCRIPT

**Characterization of domain specific Interaction of Synthesized Dye with Serum Proteins by Spectroscopic and Docking Approaches along with Determination of Invitro Cytotoxicity and Antiviral Activity**

Suparna Rudra<sup>a</sup>, Somnath Dasmandal<sup>a</sup>, Chiranjit Patra<sup>a</sup>, Biman Kumar Patel<sup>a</sup>, Suvendu Paul<sup>b</sup> and Ambikesh Mahapatra<sup>a,\*</sup>

<sup>a</sup>Department of Chemistry, Jadavpur University, Kolkata 700 032, India

<sup>b</sup>Department of Chemistry, Kalyani University, Kalyani 741235, India

**Supporting information**

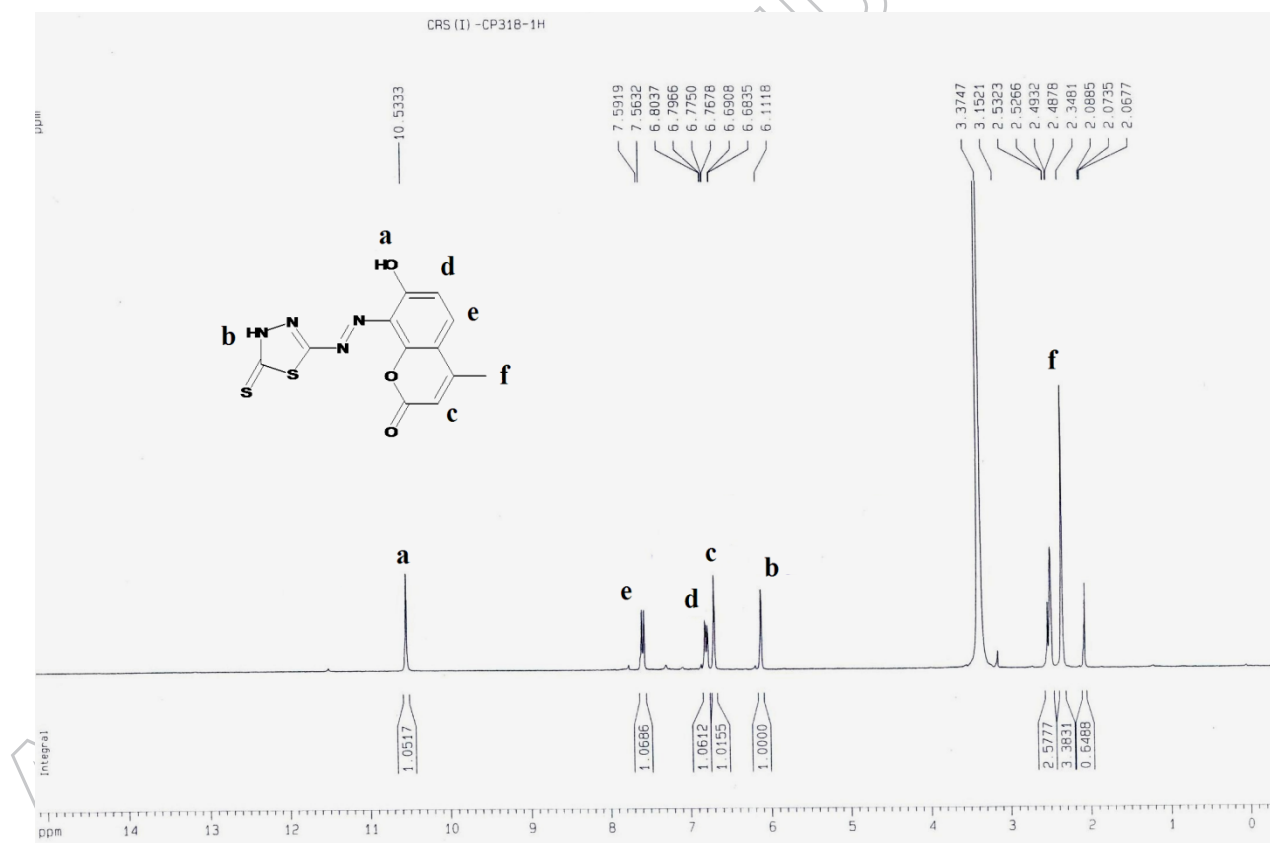


Fig. S1: <sup>1</sup>H-NMR of azo dye in DMSO-d<sub>6</sub>

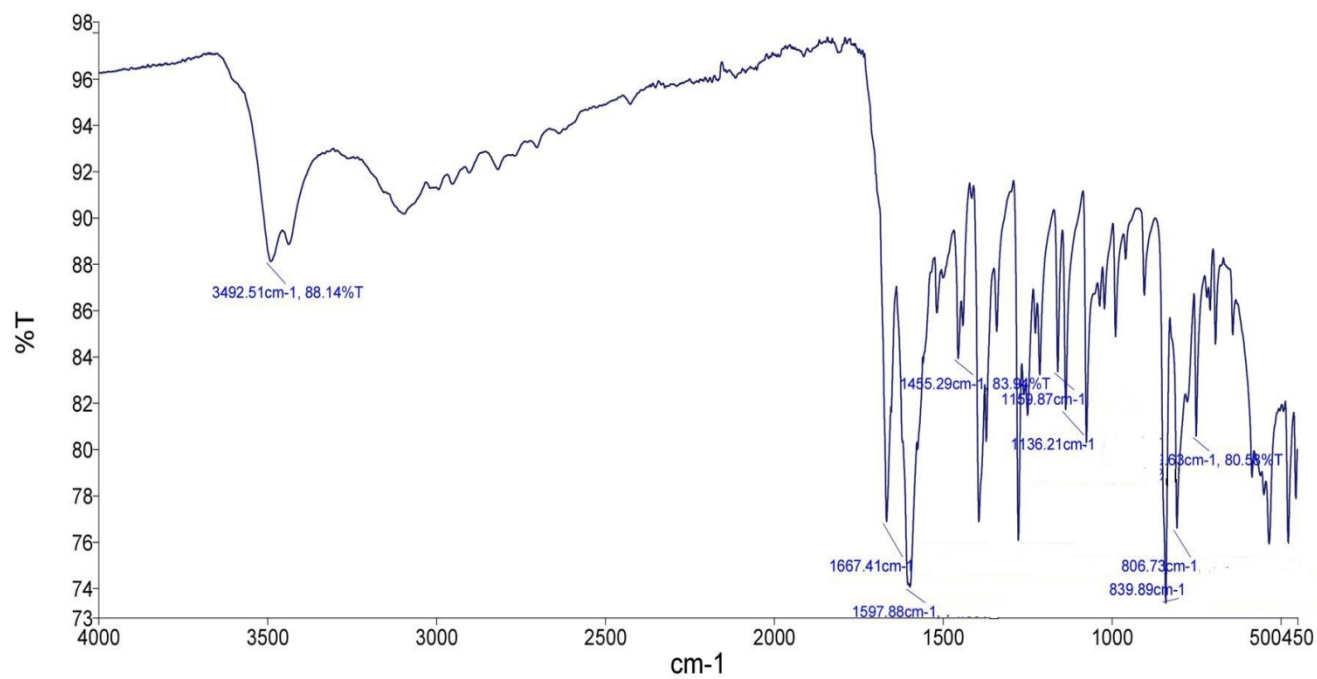


Fig. S2: IR spectrum of azo dye

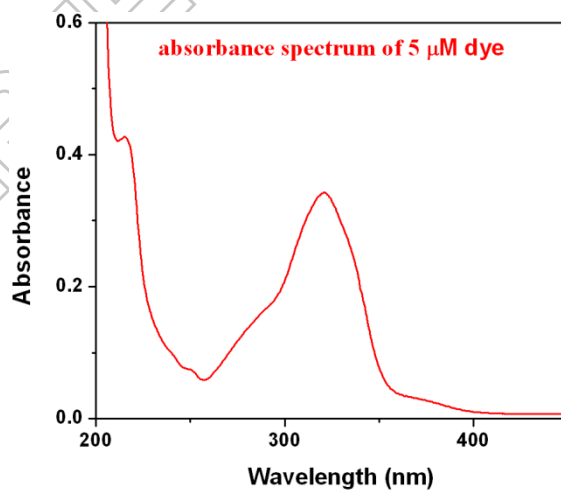


Fig. S3: Absorbance spectrum of synthesized dye

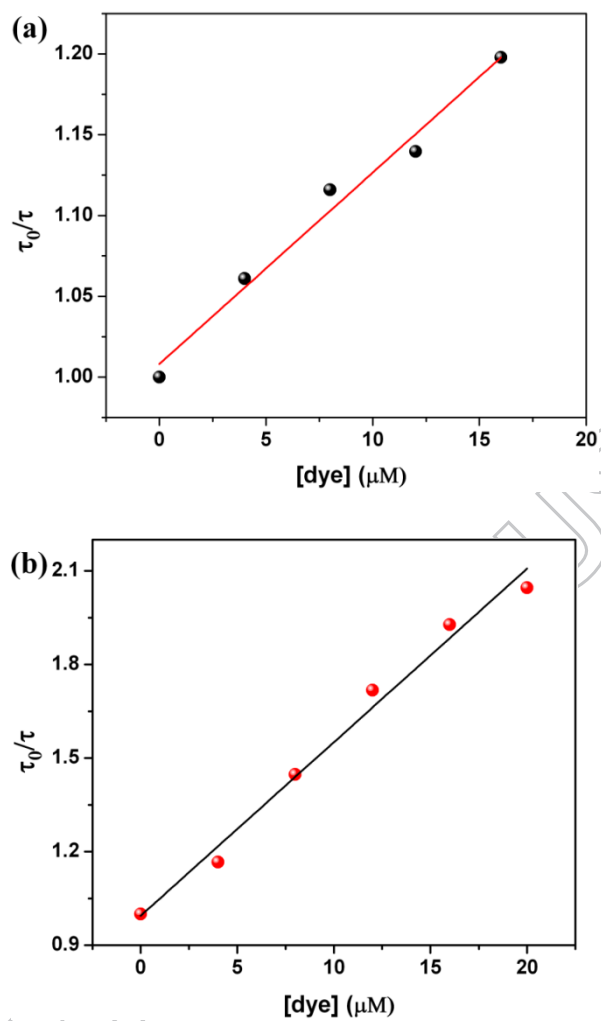
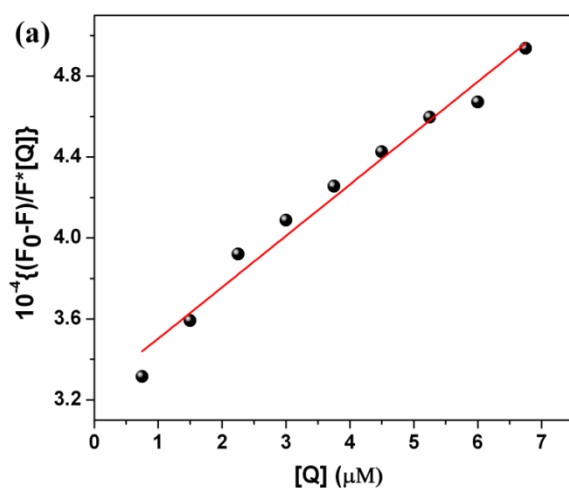


Fig. S4: Plot of  $\tau_0/\tau$  versus [dye] for (a) HSA and (b) BSA to determine the dynamic quenching constant.



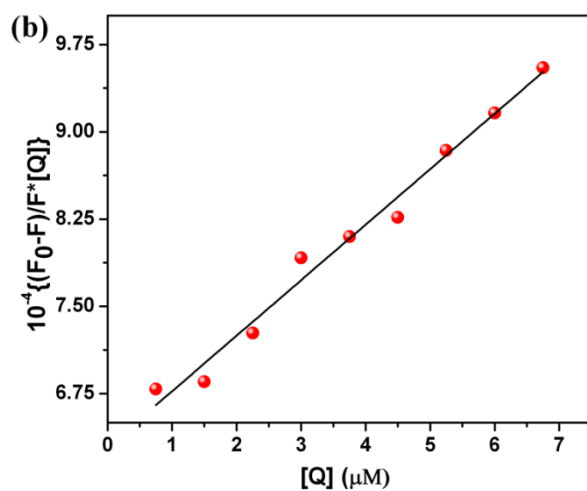
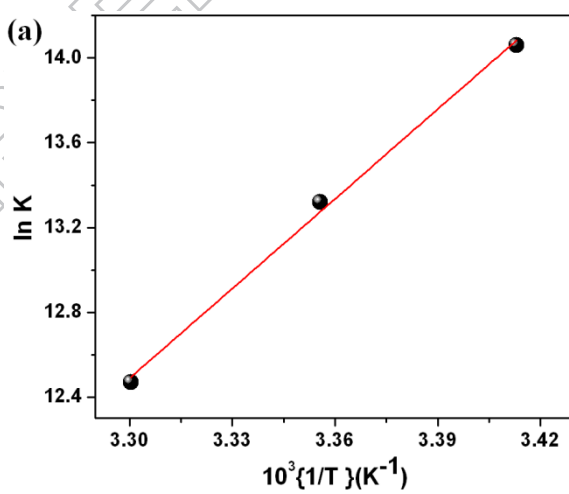


Fig. S5: Plot  $[(F_0 - F)/F]/[Q]$  versus  $[Q]$  for (a) HSA and (b) BSA



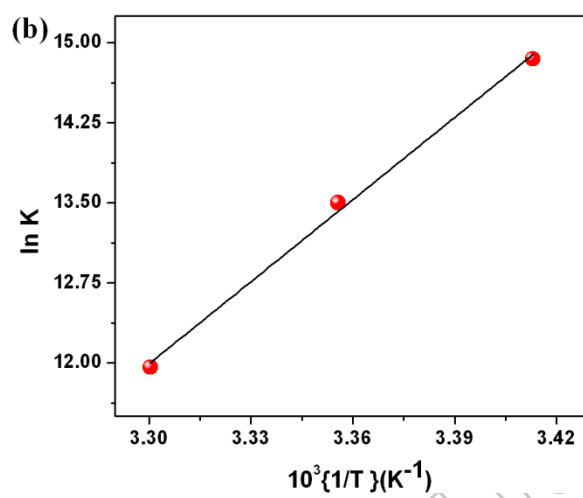


Fig. S6: van't Hoff plot for (a) HSA and (b) BSA respectively